

Charm production in relativistic heavy ion collisions

Che-Ming Ko
Texas A&M University

- Charm flow and energy loss at RHIC
- Charm production at LHC
- Charm exotics production in HIC

Collaborators: Bin Zhang (Arkansas State Univ.), Wei Liu (TAMU), Ben-wei Zhang (Huazhong Normal Univ.), Marina Nielsen (Sao Paulo), Su Houng Lee, Shigesiro Yasui (Yonsei Univ.)

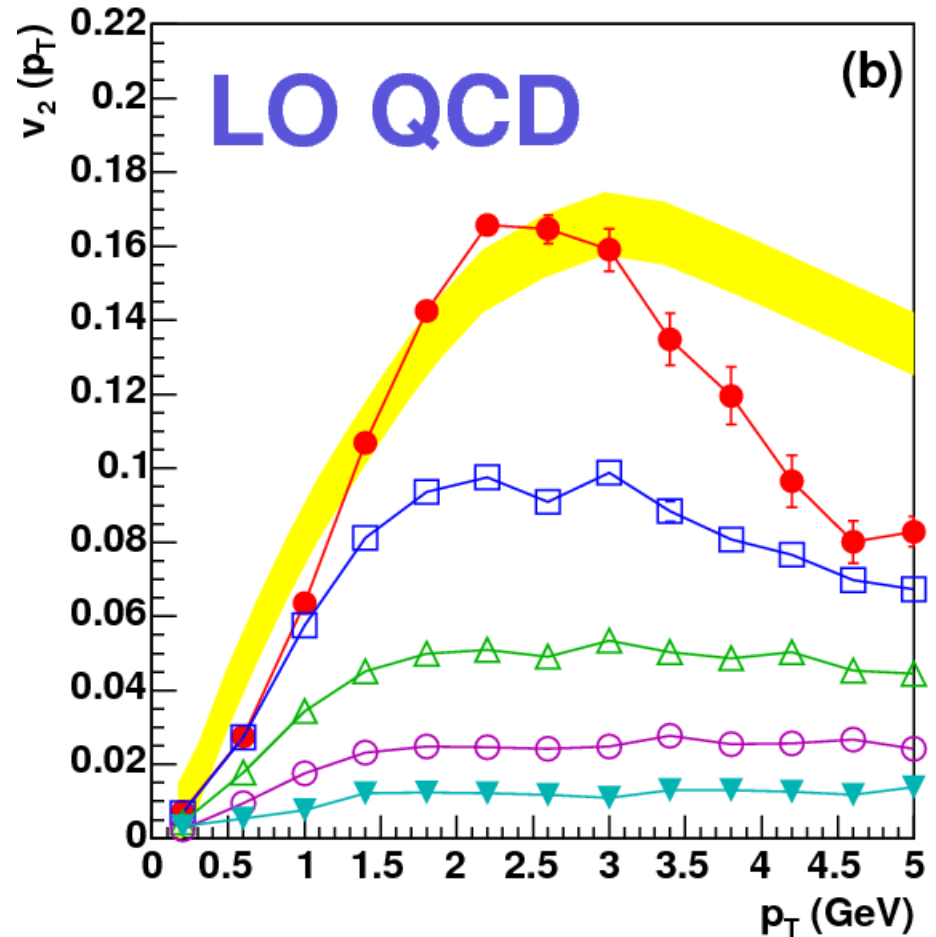
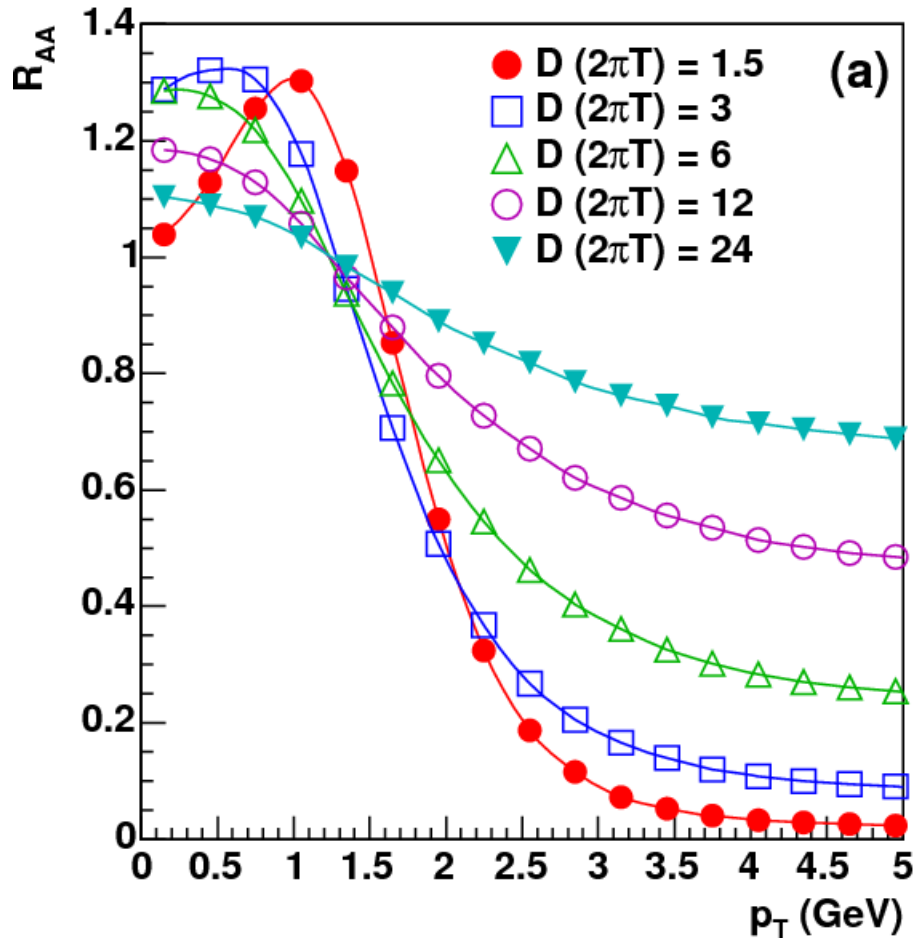
Supported by National Science Foundation and The Welch Foundation

Why is understanding charm production important in HIC?

- As a probe of charm interactions in quark-gluon plasma: More, Teaney ...
- Charmonium production: Braun-Munzinger, Thews, Greco
 - Yield depends quadratically on the charm quark number in statistical, kinetic, and coalescence models
 - Enhanced charm production would lead to possible charmonium enhancement instead of suppression, which was proposed as a signal for QGP (Matsui and Satz)
 - Expect charmonium suppression at RHIC but enhancement at LHC
- Charmed exotics production:
 - D_{sJ} (2317) as a tetraquark meson ($c\bar{s}q\bar{q}$) (Chen, Liu, Nielsen, Ko, PRC 76, 064903 (2007))
 - Consideration of the color-spin interaction leads to possible stable charmed tetraquark meson T_{cc} ($ud\bar{c}\bar{c}$) and pentaquark baryon Θ_{sc} ($udus\bar{c}$) (Lee, Yasui, Liu & Ko (hep-ph/0707.1747))
 - Enhanced charm production at LHC makes the latter a possible factory for studying charmed exotics

Charm elliptic flow from the Langevin model

Moore & Teaney, PRC 71, 064904 (2005)



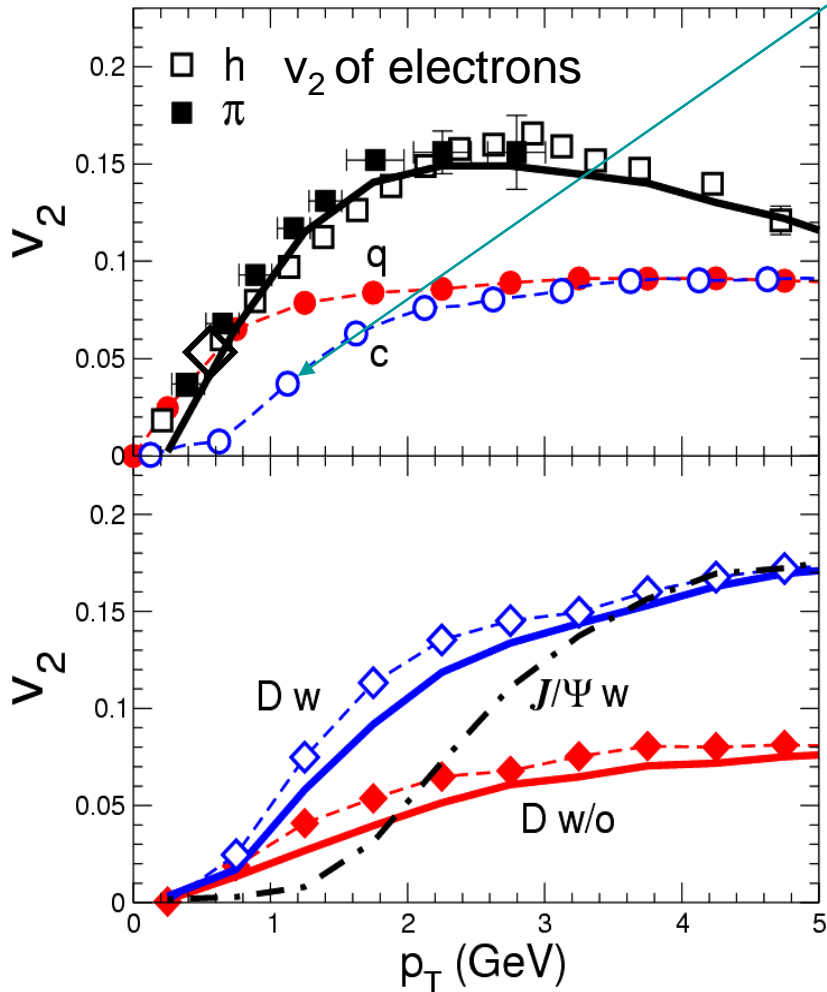
pQCD gives $D \approx a/(2\pi T)$ in QGP with $a=6$

Charmed meson elliptic flow

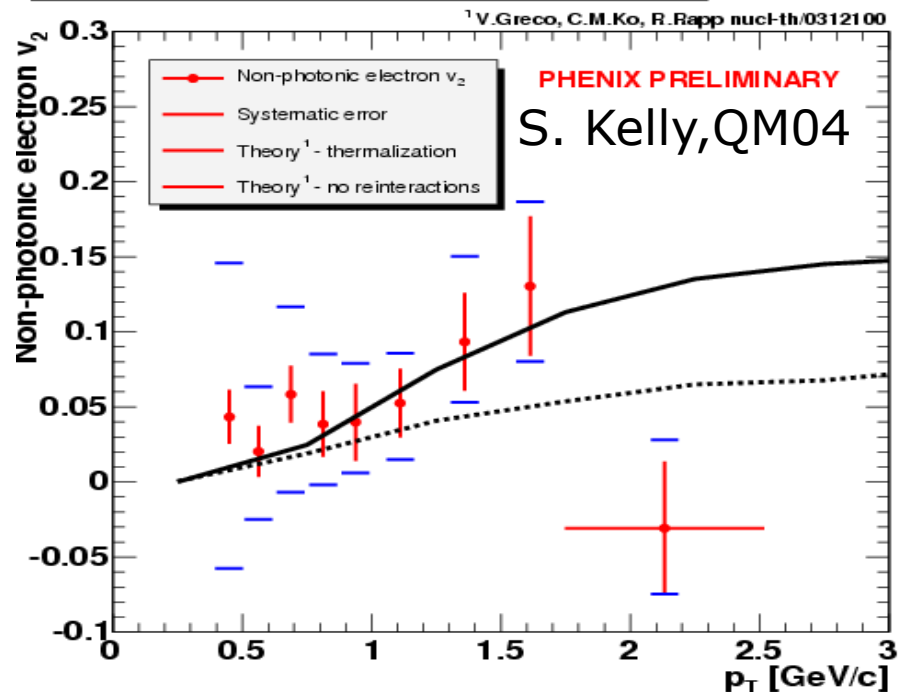
Greco, Rapp, Ko, PLB595, 202 (04)

Quark coalescence

Smaller charm v_2 than light quark v_2 at low p_T due to mass effect



Single electron invariant p_T distribution



Data consistent with thermalized charm quark with same v_2 as light quarks

A multiphase transport (AMPT) model

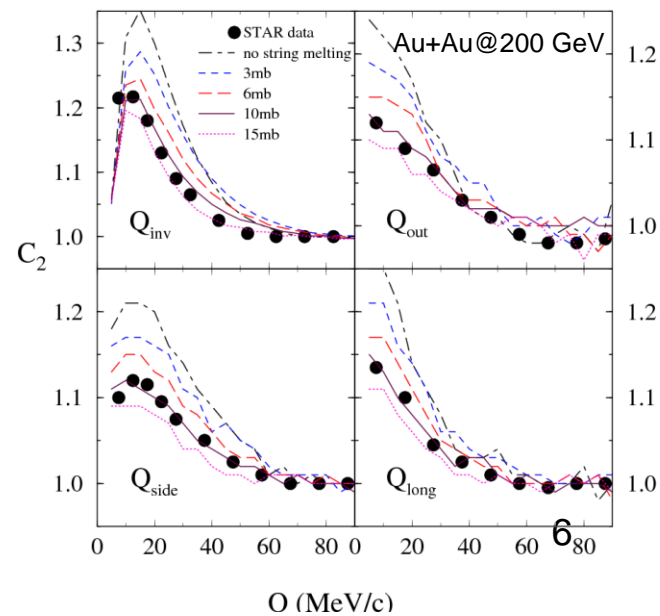
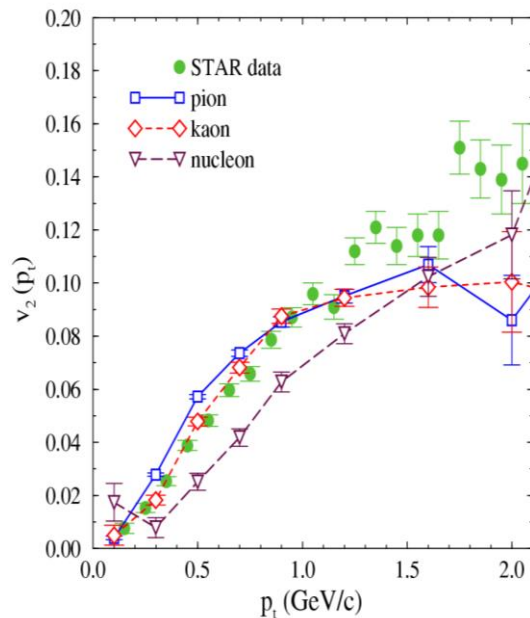
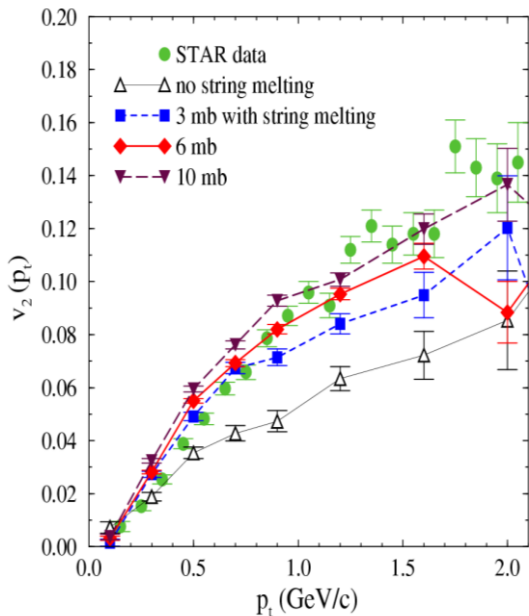
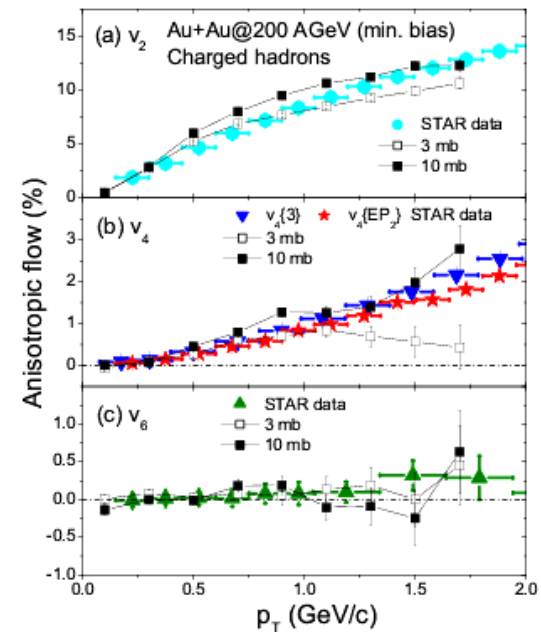
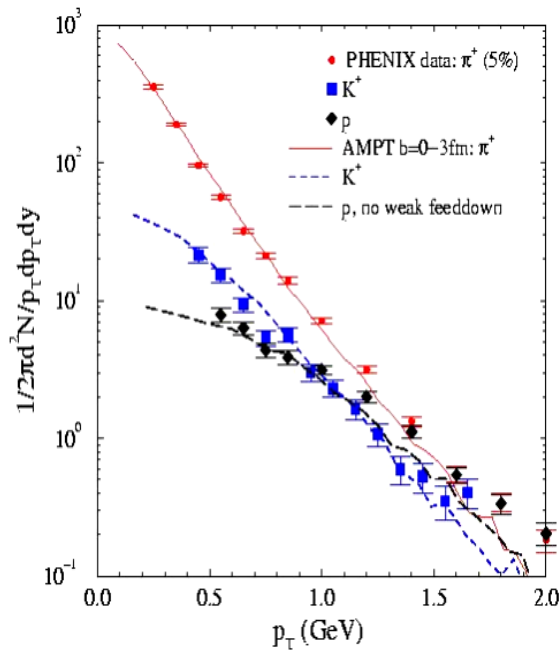
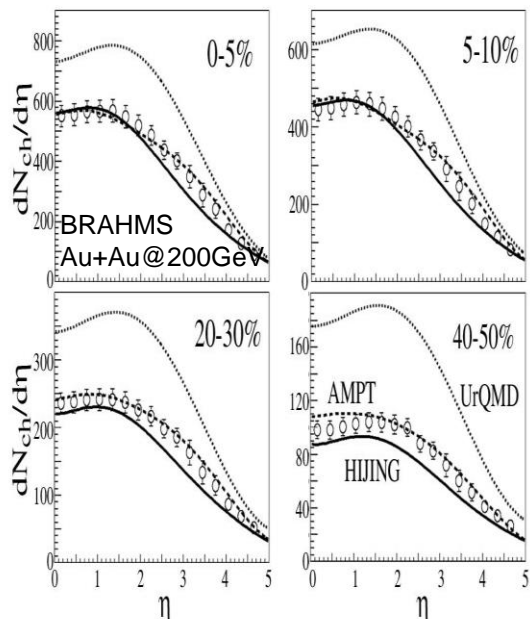
Default: Lin, Pal, Zhang, Li & Ko, PRC 61, 067901 (00); 64, 041901 (01);
72, 064901 (05); <http://www.cunuke.phys.columbia.edu/OSCAR>

- Initial conditions: HIJING (soft strings and hard minijets)
- Parton evolution: ZPC
- Hadronization: Lund string model for default AMPT
- Hadronic scattering: ART

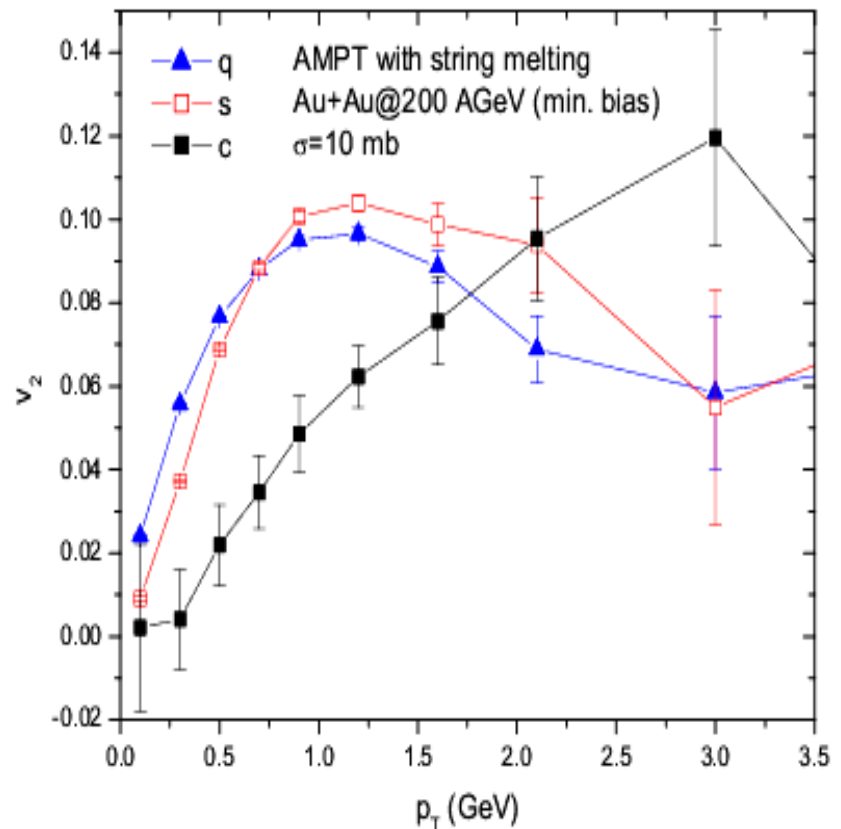
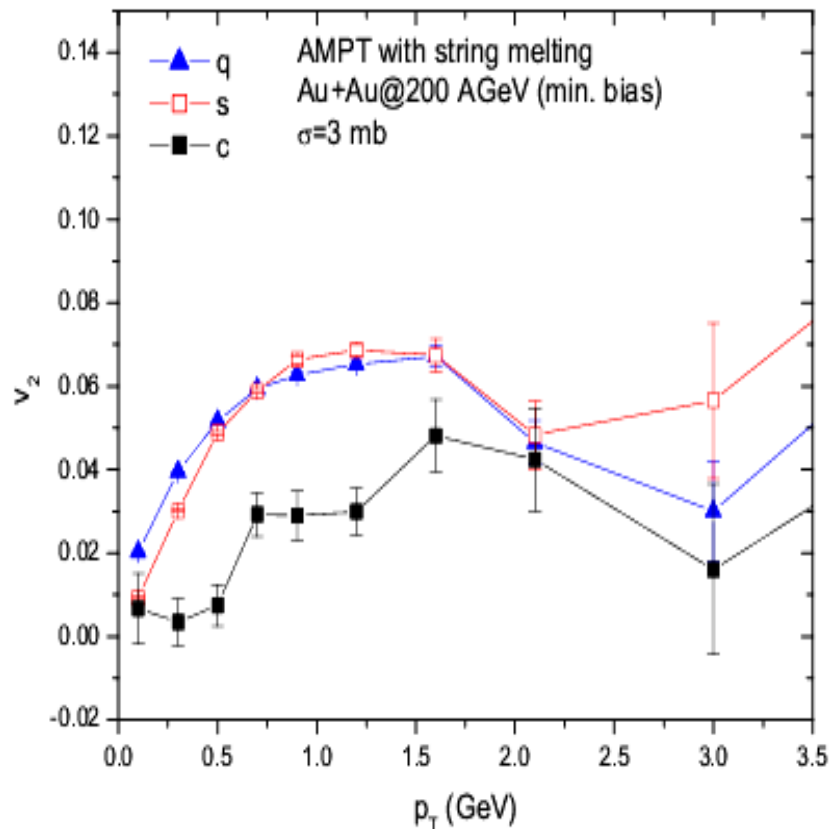
String melting: PRC 65, 034904 (02); PRL 89, 152301 (02)

- Convert hadrons from string fragmentation into quarks and antiquarks
- Evolve quarks and antiquarks in ZPC
- When partons stop interacting, combine nearest quark and antiquark to meson, and nearest three quarks to baryon (coordinate-space coalescence)
- Hadron flavors are determined by quarks' invariant mass

Results from AMPT for RHIC



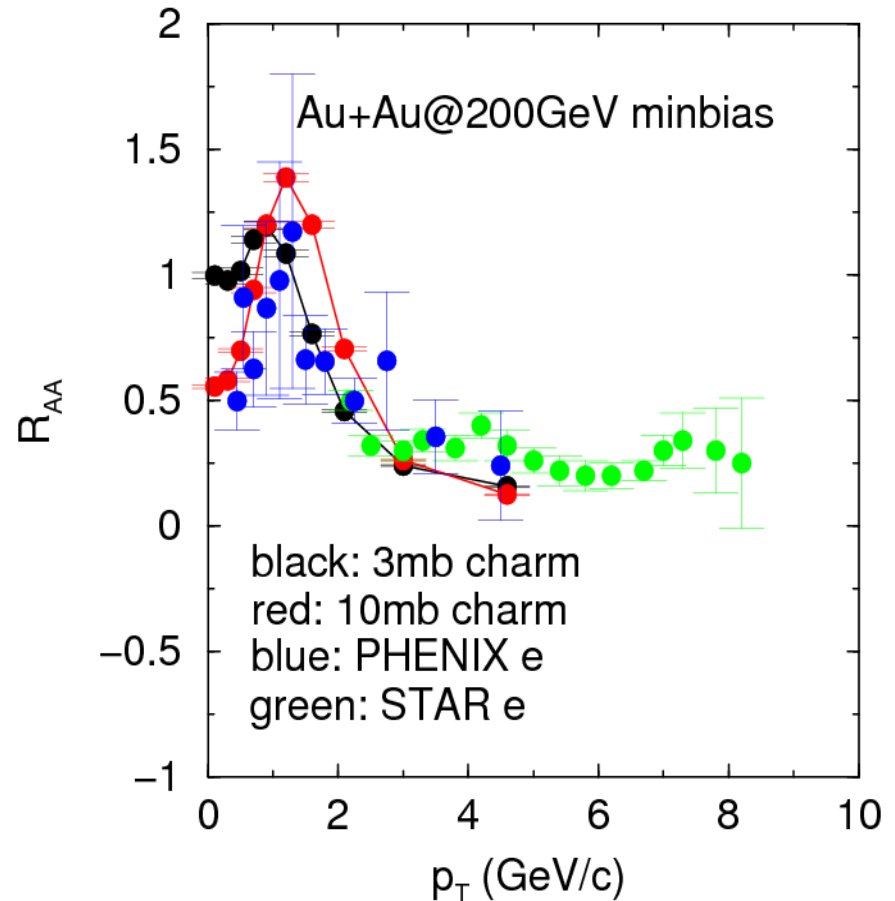
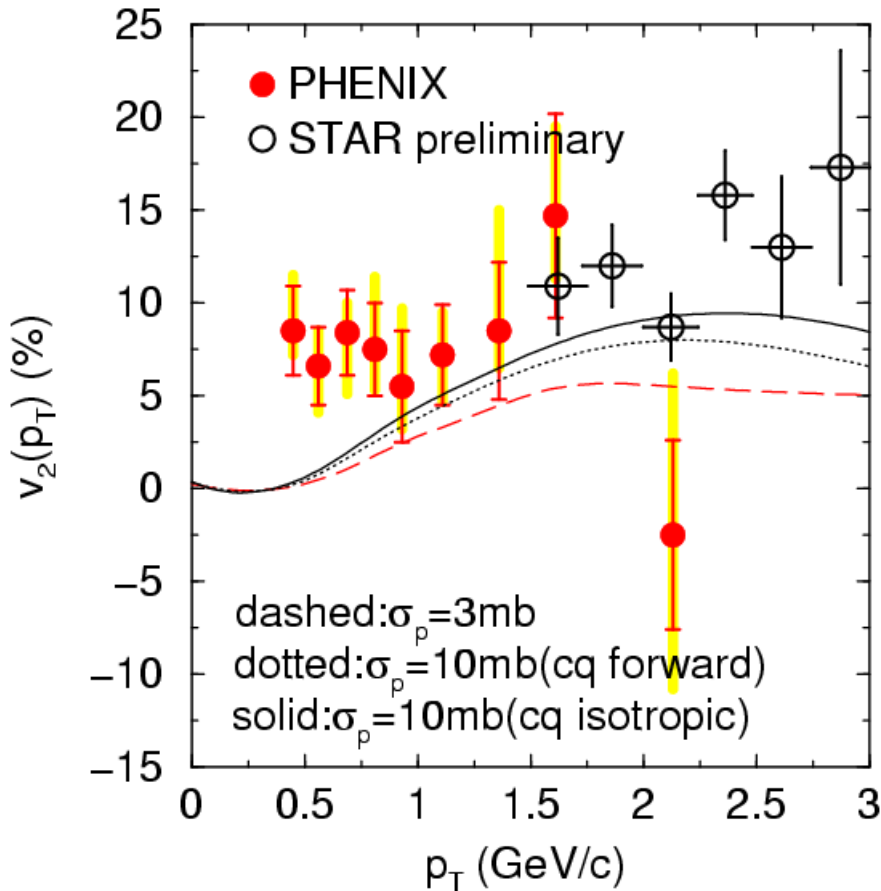
Charm quark elliptic flow from AMPT



- P_T dependence of charm quark v_2 is different from that of light quarks
- At high p_T , charm quark has similar v_2 as light quarks
- Charm elliptic flow is also sensitive to parton cross sections

Charm R_{AA} and elliptic flow from AMPT

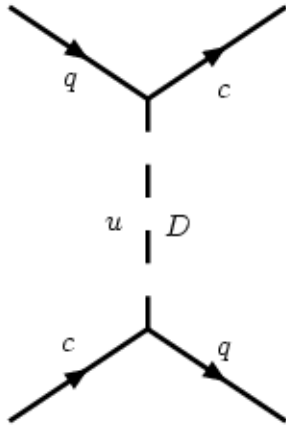
Zhang, Chen & Ko, PRC 72, 024906 (05)



- Need large charm scattering cross section to explain data
- Smaller charmed meson elliptic flow is due to use of current light quark masses

Resonance effect on charm scattering in QGP

Van Hees & Rapp, PRC 71, 034907 (2005)



$$\sigma_{c\bar{q} \rightarrow c\bar{q}} = \frac{1}{9} \frac{2J+1}{4} \frac{\pi}{k^2} \frac{\Gamma_D^2}{(s^{1/2} - m_D)^2 + \Gamma_D^2/4}$$

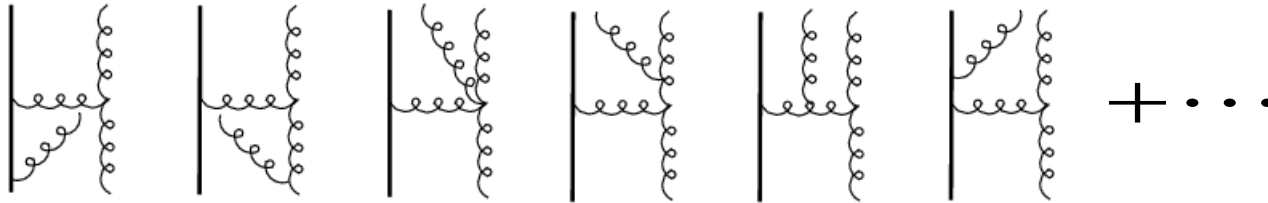
With $m_c \approx 1.5$ GeV, $m_q \approx 5-10$ MeV, $m_D \approx 2$ GeV, $\Gamma_D \approx 0.3-0.5$ GeV, and including scalar, pseudoscalar, vector, and axial vector D mesons gives

$$\sigma_{cq \rightarrow cq}(s^{1/2} = m_D) \approx 6 \text{ mb}$$

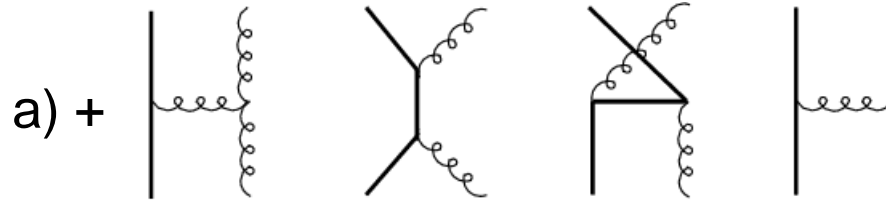
Since the cross section is isotropic, the transport cross section is 6 mb, which is about 4 times larger than that due to pQCD t-channel diagrams, leading to a charm quark drag coefficient $\gamma \sim 0.16$ c/fm in QGP at $T=225$ MeV.

Heavy quark energy loss in pQCD

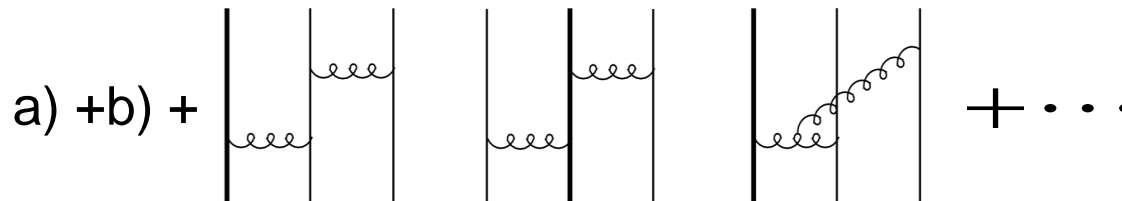
a) Radiative energy loss (Amesto *et al.*, hep-ph/0511257)



b) Radiative and elastic energy loss (Wicks *et al.*, nucl-th/0512076)

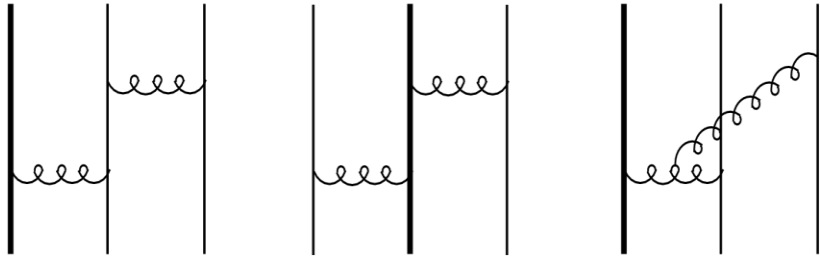


c) Three-body elastic scattering (Liu & Ko, nucl-th/0603004)

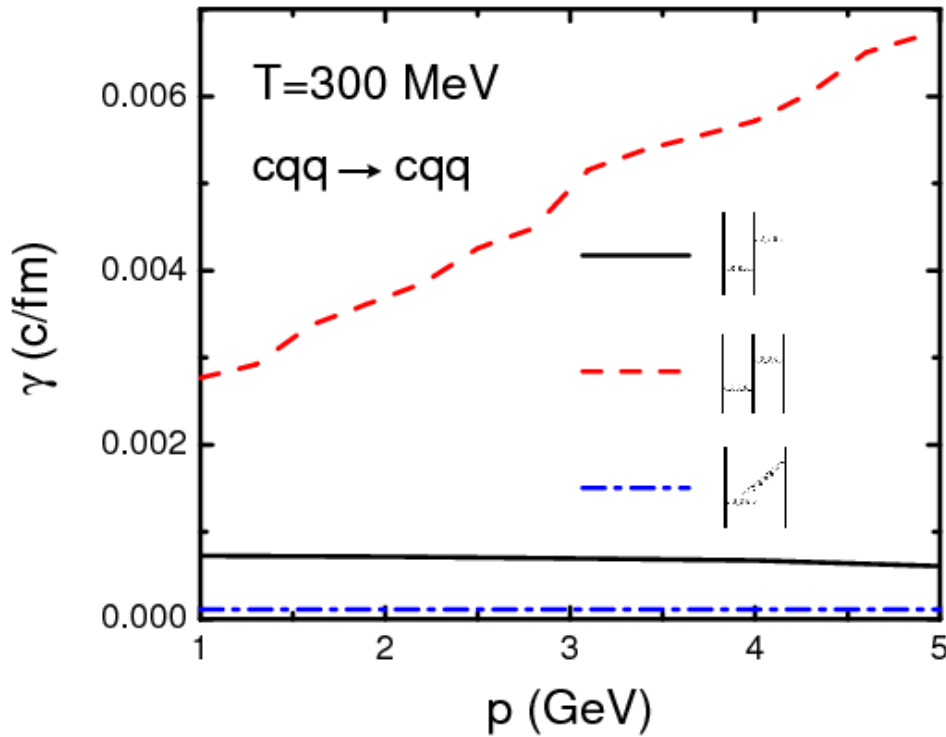


- May be important as interparton distance \sim range of parton interaction
- At $T=300$ MeV, $N_g \sim (N_q + N_{qbar}) \sim 5/\text{fm}^3$, so interparton distance ~ 0.3 fm
- Screening mass $m_D = gT \sim 600$ MeV, so range of parton interaction ~ 0.3 fm

1) $Qqq \rightarrow Qqq$, $Qq\bar{q} \rightarrow Qq\bar{q}$, $Q\bar{q}q \rightarrow Q\bar{q}q$ with different flavors
(7 diagrams)



Drag coefficient $\gamma(|\mathbf{p}|) = \langle 1 \rangle - \frac{\langle \mathbf{p} \cdot \mathbf{p}' \rangle}{|\mathbf{p}|^2}$



True 3-body interaction requires intermediate quark to be off shell, achieved by taking the real part of its propagator after including its collisional width

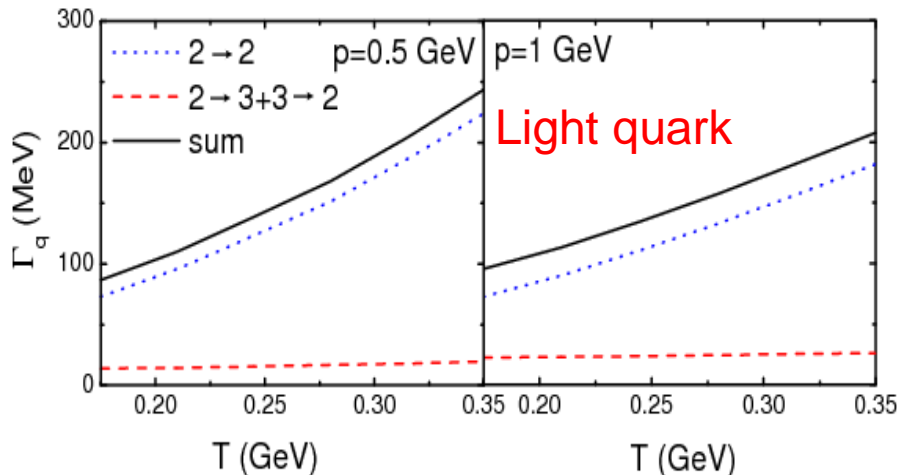
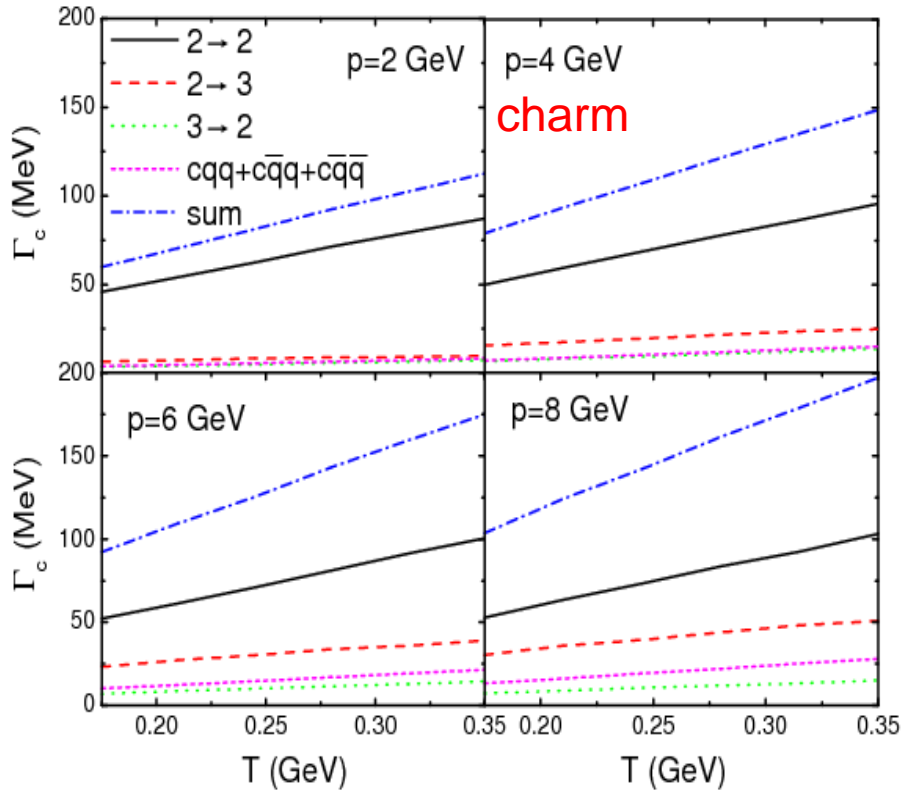
$$m_{Q,q} \rightarrow m_{Q,q} + i \frac{\Gamma_{Q,q}}{2}$$

Screening mass $m_D = gT$

Thermal mass $m_g = \sqrt{3}m_q = \frac{m_D}{\sqrt{2}}$

Dominated by diagram with two gluons attached to heavy quark. Not surprising as other diagrams can be considered as medium modification of light quarks and gluons.

Collisional width of quarks in QGP



$$\Gamma_{Q,q} = \hbar \sum_i \left\langle |\mathbf{M}_i|^2 \right\rangle$$

$$\begin{aligned} & \left\langle |\mathbf{M}_{i_1 \dots i_m \rightarrow j_1 \dots j_n}|^2 \right\rangle \\ &= \frac{1}{2E_{i_1}} \prod_{k=2, \dots, m} \int \frac{g_{i_k} d^3 p_{i_k}}{(2\pi)^3 2E_{i_k}} \prod_{l=1, \dots, n} \int \frac{d^3 p_{j_l}}{(2\pi)^3 2E_{j_l}} \\ & \times \prod_{k=2, \dots, m} f(p_{i_k}) \prod_{l=2, \dots, n} \overline{1 \pm f(p_{j_l})} \left| \mathbf{M}_{i_1 \dots i_m \rightarrow j_1 \dots j_n} \right|^2 \\ & \times (2\pi)^4 \delta^{(4)} \left(\sum_{k=1, \dots, m} p_{i_k} - \sum_{l=1, \dots, n} p_{j_l} \right) \end{aligned}$$

With $\alpha_s = g^2/4\pi = 0.3$, quark collisional widths are mainly due to 2-body elastic scattering. Width of bottom quark is about two thirds of that of charm quark.

2) $Qqq \rightarrow Qqq, Q\bar{q}\bar{q} \rightarrow Q\bar{q}\bar{q}$ with same flavor

7 extra diagrams due to interchange of final two light quarks. Give same contribution as that due to direct diagrams. Interference terms are two orders of magnitude smaller.

3) $Qq\bar{q} \rightarrow Qq\bar{q}$ with same flavor

5 extra diagrams from exchanging a gluon between heavy quark and light quark, antiquark, or gluon in quark and antiquark annihilation. Contribution is two order of magnitude smaller than that due to direct diagrams.

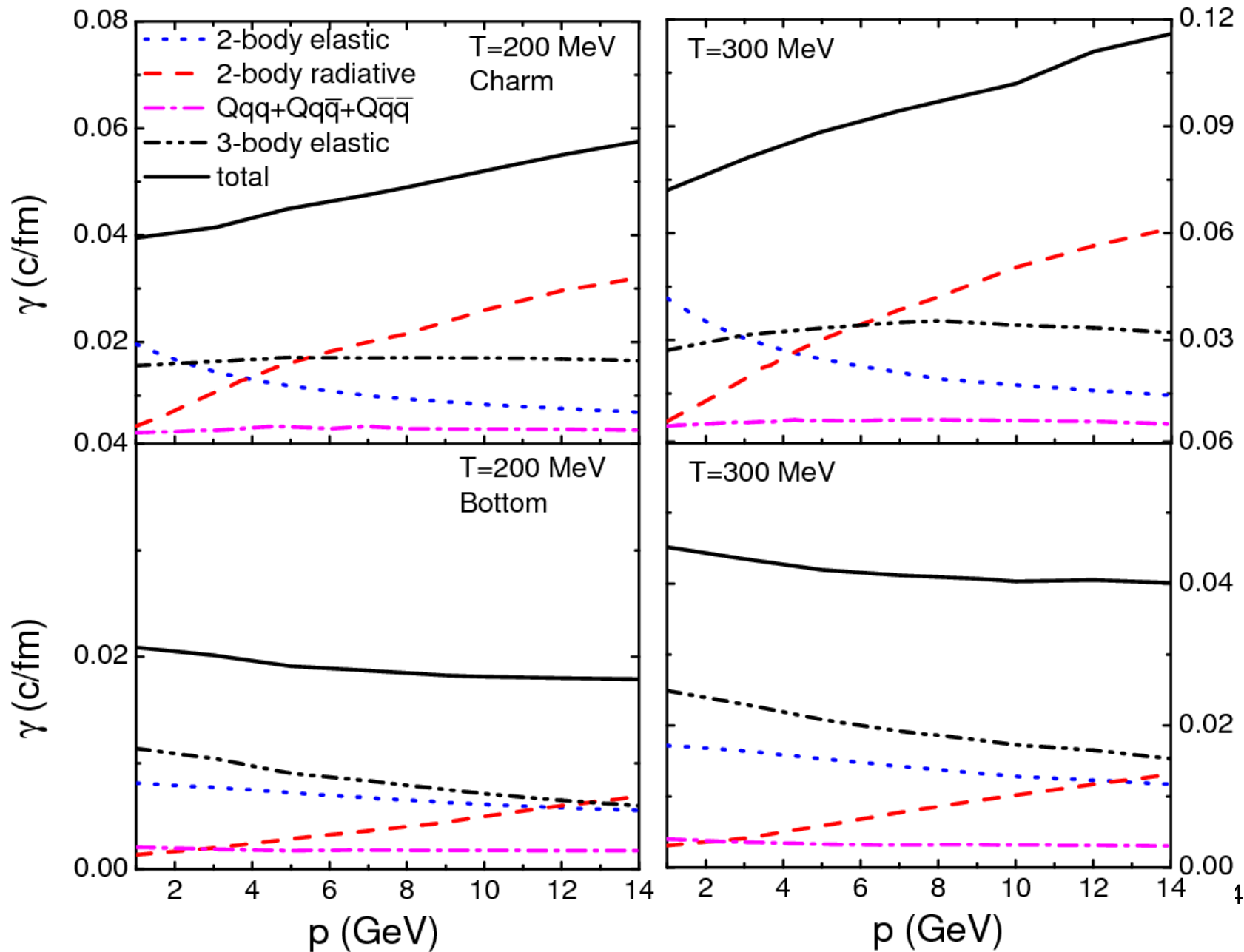
4) $Qqg \rightarrow Qqg$ and $Q\bar{q}g \rightarrow Q\bar{q}g$

36 diagrams obtained by attaching an extra gluon to all parton lines and three-gluon vertices in $Qq \rightarrow Qqg$. Only two diagrams with two gluons attached to heavy quark have been evaluated.

5) $Qgg \rightarrow Qgg$

123 diagrams obtained from $Qg \rightarrow Qgg$ by attaching an extra gluon. Only two diagrams with two gluons attached to heavy quark have been calculated.

Heavy quark drag coefficients in QGP



Heavy quark momentum degradation in QGP

Fokker-Planck equation \rightarrow
$$\frac{d\langle p_T \rangle}{dt} = -\langle \gamma(p_T, T) p_T \rangle$$

Using
$$\gamma(p_T, T) \approx \gamma_0(T)(1+ap_T), \quad \langle p_T^2 \rangle \approx \langle p_T \rangle^2$$

then
$$\langle p_T \rangle = \frac{B}{1-aB}$$
 with
$$B = \frac{p_0 \exp\left(-\int_{\tau_0}^{\tau_f} \gamma_0(\tau) d\tau\right)}{1+ap_0}$$

τ_f : smaller of the time when QGP ends and the time when heavy quark escapes the expanding QGP fireball.

QGP fireball dynamics:
$$V(\tau) = \pi \tau \left[R_0 + \frac{a}{2} (\tau - \tau_0)^2 \right]$$
 $T(\tau)$ from entropy conservation

$R_0 = 7$ fm, $\tau_0 = 0.6$ fm, $a = 0.1$ c²/fm

$T_i = 350$ MeV, $T_c = 175$ MeV @ $\tau_c = 5$ fm

Appropriate for central
Au+Au @ 200 AGeV

Initial heavy quark spectra

Charm quarks: from fitting simultaneously measured spectrum of charm mesons from d+Au collisions and of electrons from heavy meson decays in p+p collisions.

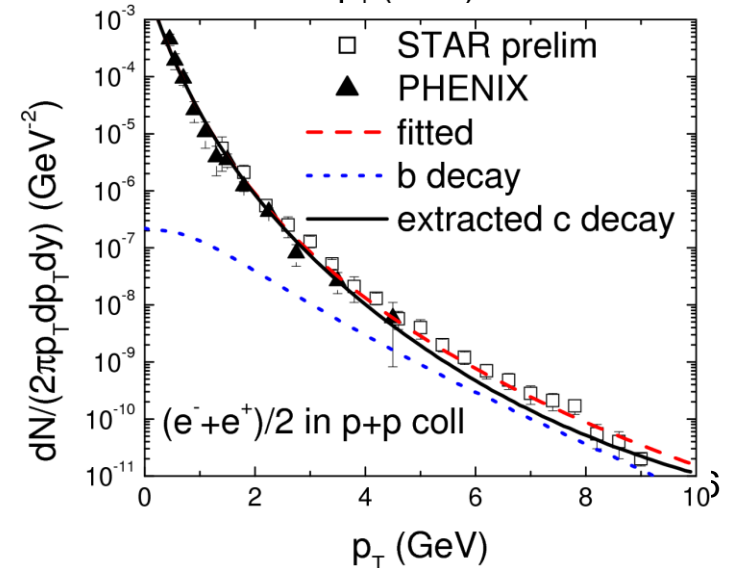
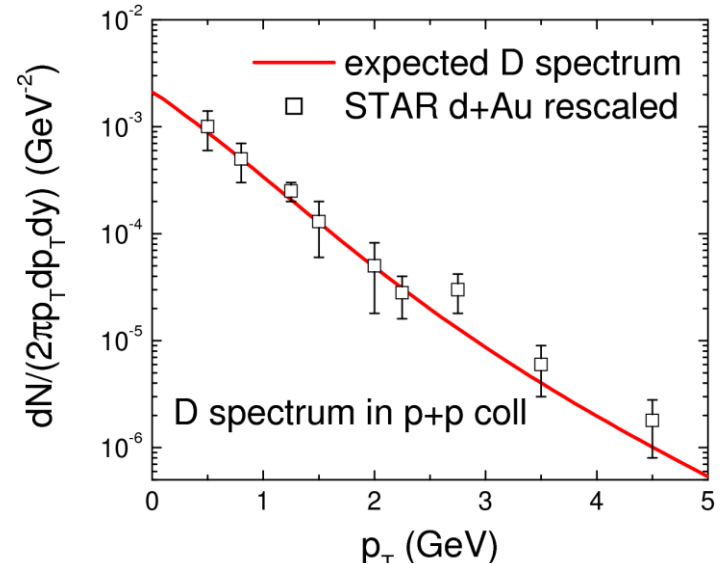
$$\frac{dN_c}{d^2 p_T} = N_{\text{coll}} \frac{dN_c^{\text{pp}}}{d^2 p_T}$$

$$= \frac{19.2 \left[1 + \left(\frac{p_T}{6} \right)^2 \right]}{\left(1 + p_T/3.7 \right)^{12} \left[1 + \exp(0.9 - 2p_T) \right]}$$

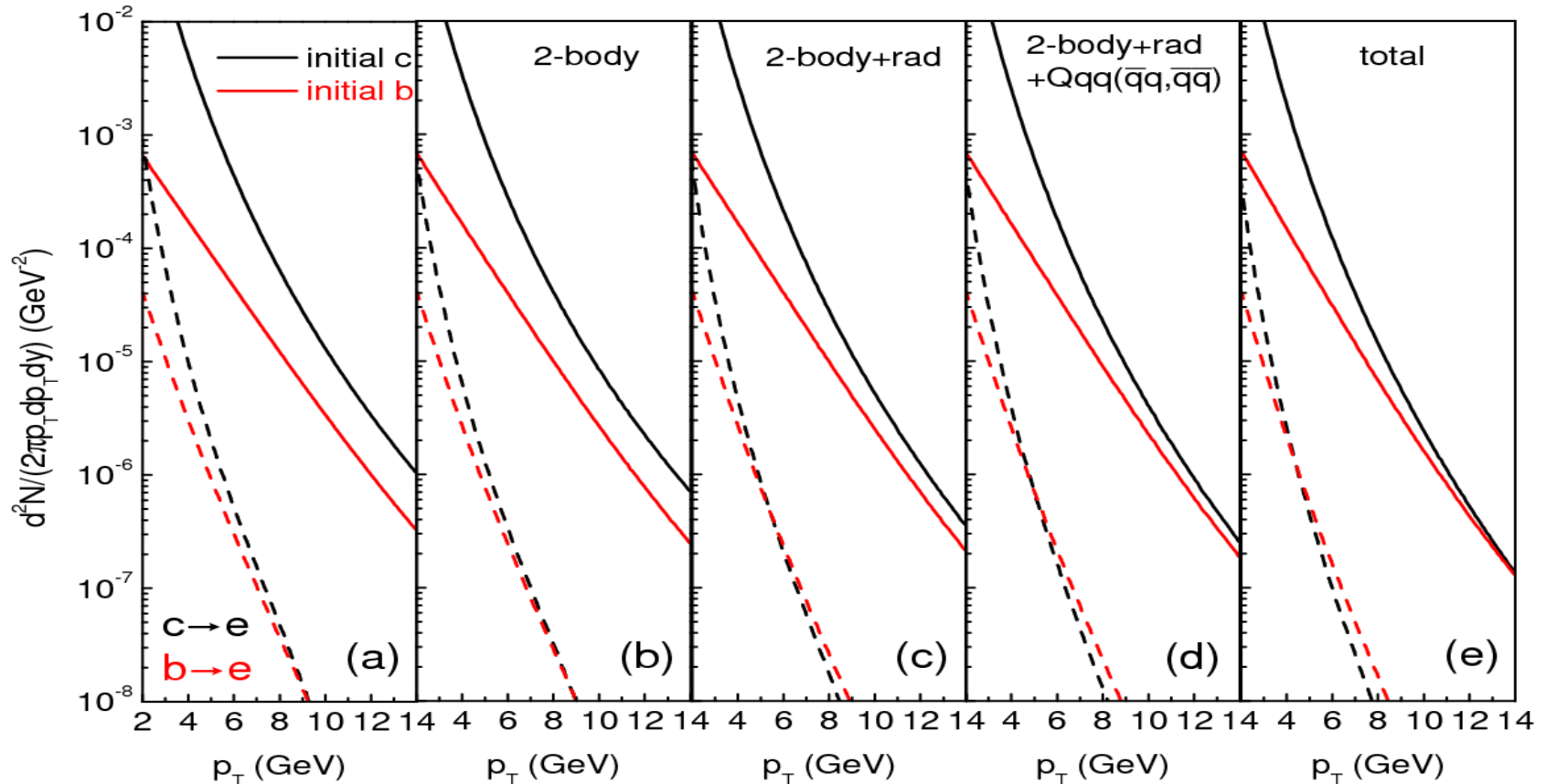
Bottom quarks: from the upper limit of uncertainty band of pQCD prediction

$$\frac{dN_b}{d^2 p_T} = N_{\text{coll}} \frac{dN_b^{\text{pp}}}{d^2 p_T}$$

$$= 0.0025 \left[1 + \left(\frac{p_T}{16} \right)^5 \right] \exp\left(-\frac{p_T}{1.495}\right)$$



Heavy quark and decay electron spectra



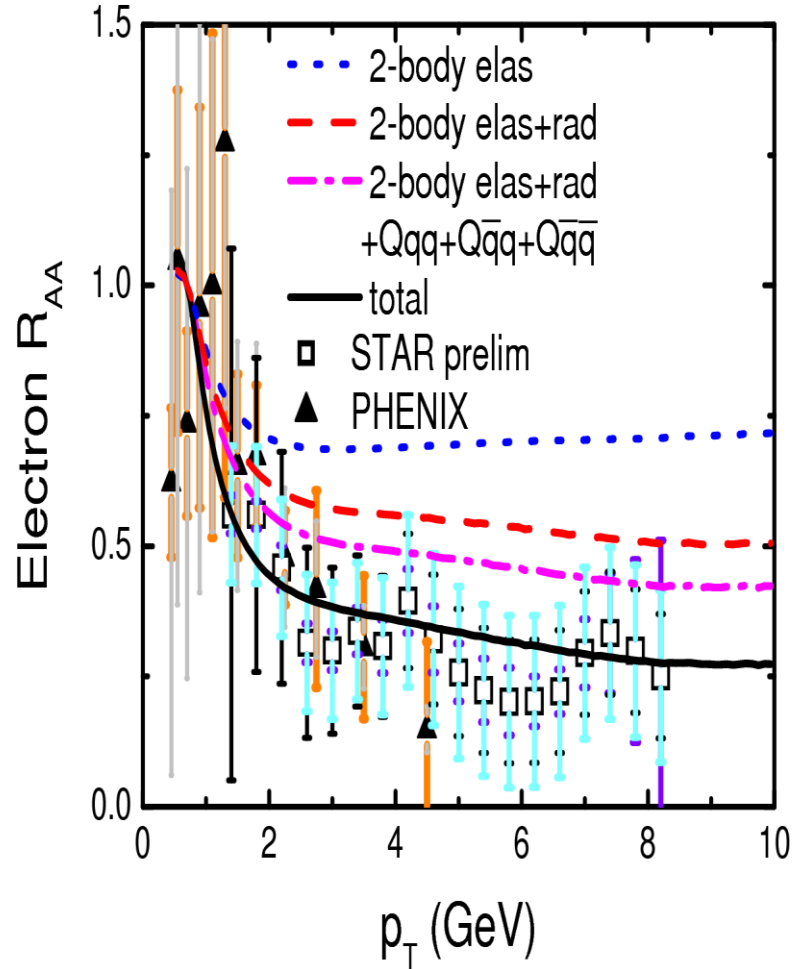
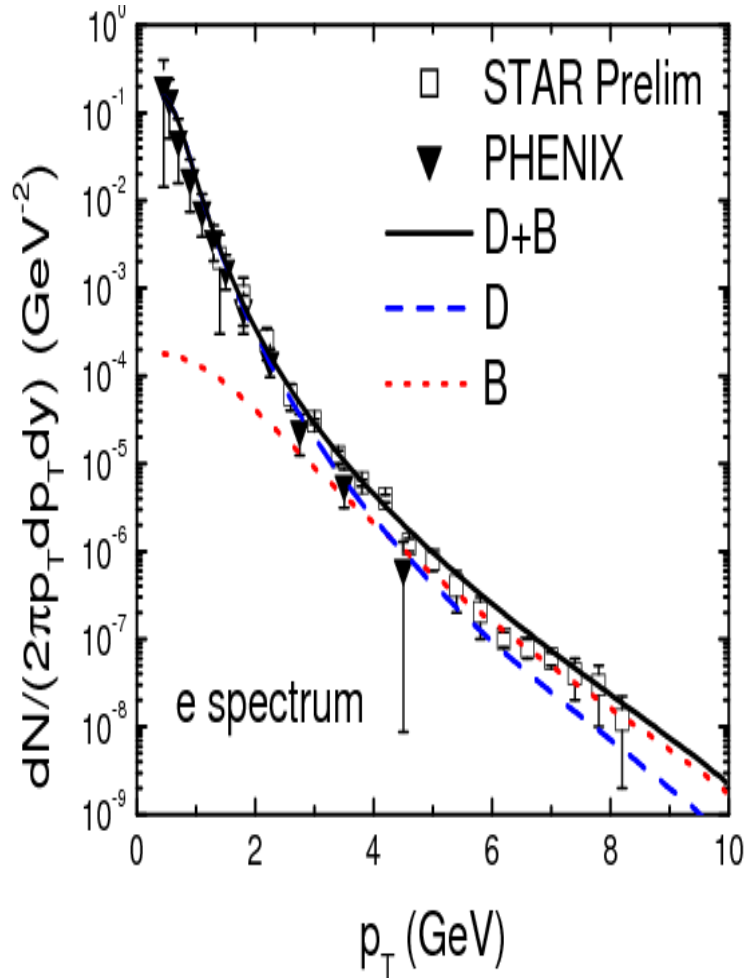
Peterson fragmentation function is used to fragment heavy quarks to heavy mesons

e

$$D(z) = \frac{1}{z[1-1/z-\epsilon/(1-z)]^2}$$

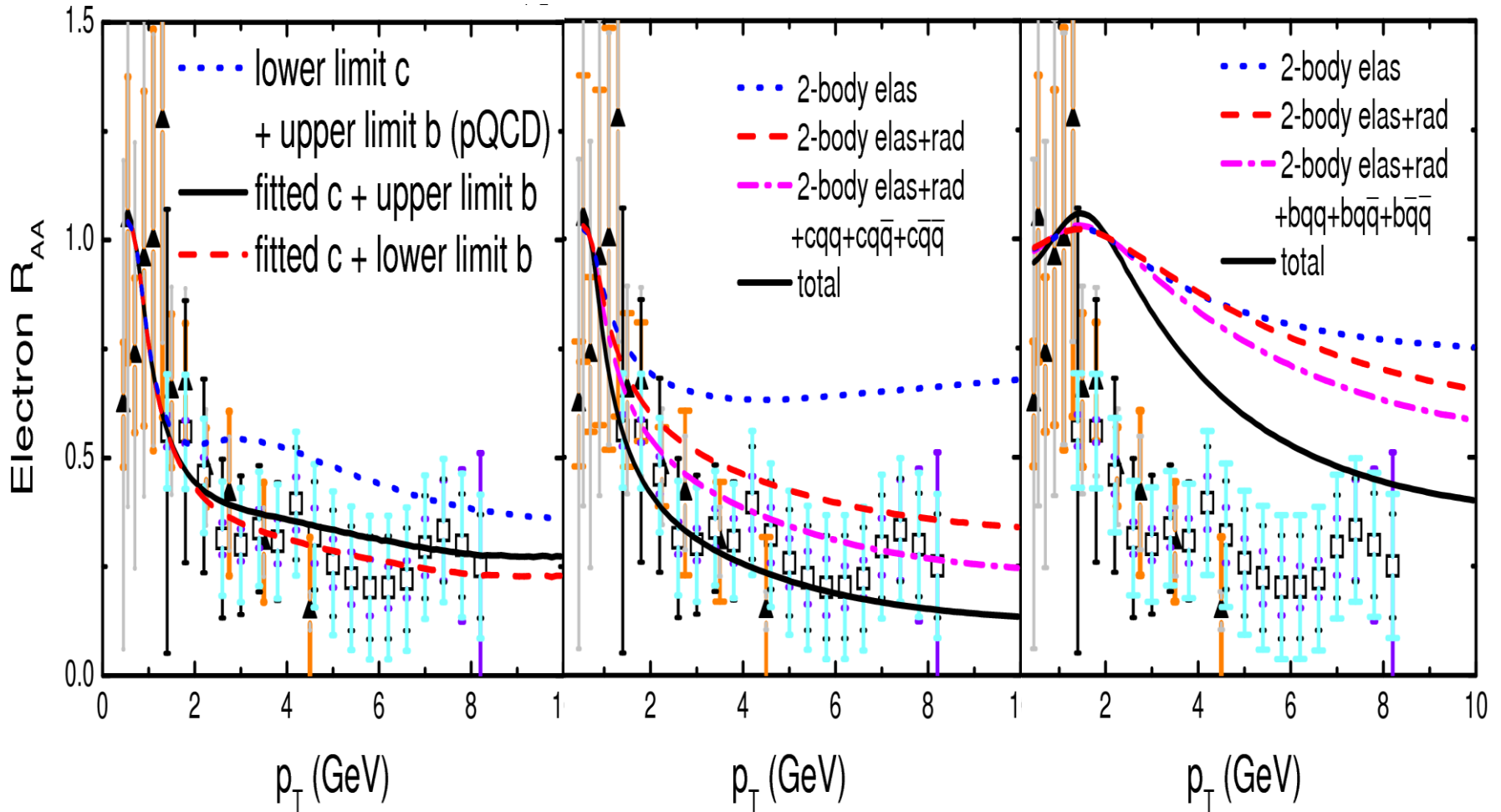
$$\epsilon_D = 0.02, \epsilon_B = 0.002$$

Spectrum and nuclear modification factor of electrons from heavy meson decay



Reasonable agreement with data from Au+Au @ 200A GeV after including heavy quark three-body scattering.

Other scenarios



Summary I

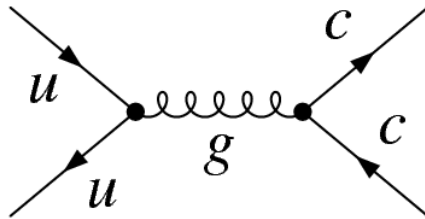
- Heavy quark three-body scattering in QGP is important: comparable to both two-body elastic and radiative scattering for charm quarks; dominant for bottom quarks.
- Including three-body scattering helps to explain observed nuclear modification factor of electrons from heavy meson decays.
- More accurate evaluation of three-body scattering is required.
- Method for resumming multi-body scattering effect needs to be developed.
- Three-body scattering of gluon and light quark jets need to be studied.

Four stages of charm production in HIC

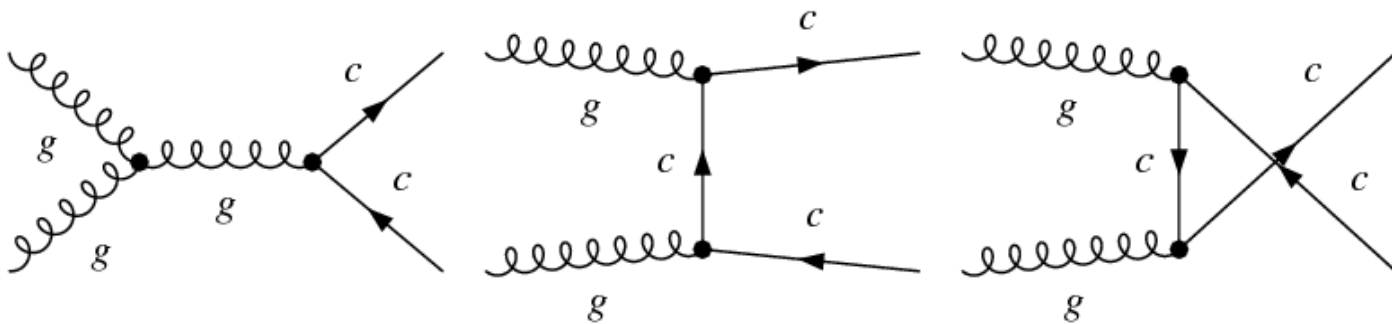
- Direct production: Mueller, Wang (92); Vogt (94); Gavin (96)
 - Mainly from initial gluon fusions
 - About 3 pairs in mid-rapidity at RHIC (from STAR collaboration)
 - About 20 pairs in mid-rapidity at LHC
- Pre-thermal production: Lin, Gyulassy (95), Levai, Mueller, Wang (95).....
 - Not important based on minijet gluons
 - Production from initial strong color field?
- Thermal production from QGP: Levai, Vogt (97)
 - Based on leading-order calculations
 - Important if initial temperature of QGP is high
- Thermal production from hadronic matter: Cassing et al. (99), Liu & Ko (02)
 - Such as $\pi N \rightarrow \Lambda_c D$ and $p N \rightarrow \Lambda_c D$
 - Expect small effect on charm production in HIC

Leading-order diagrams for charm production

1) $q\bar{q} \rightarrow c\bar{c}$

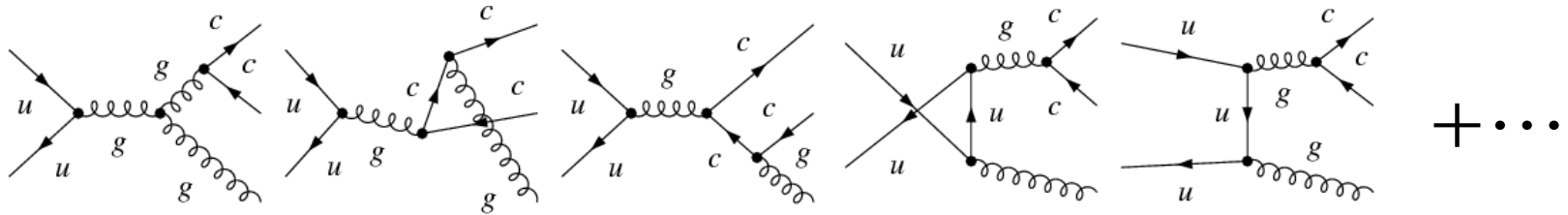


2) $gg \rightarrow c\bar{c}$

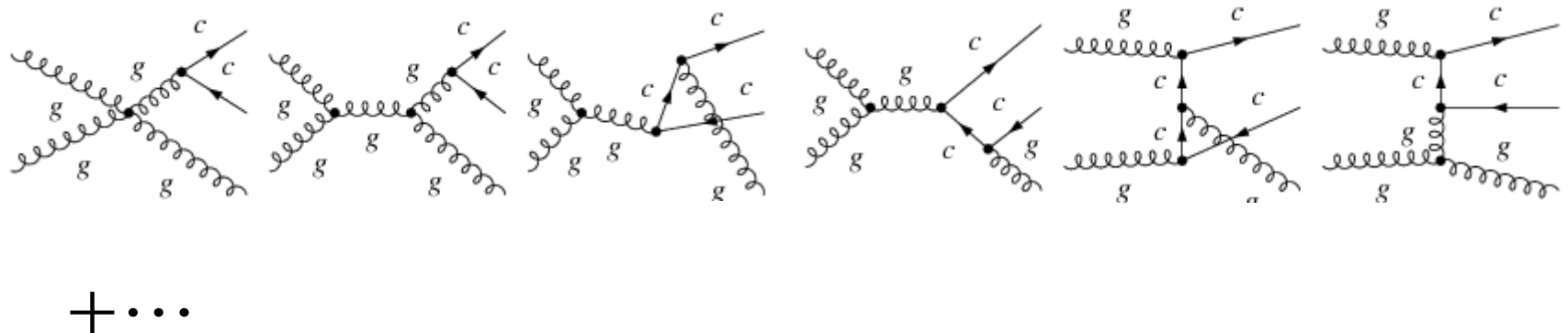


Next-Leading-order diagrams for charm production

1) $q\bar{q} \rightarrow c\bar{c}g$

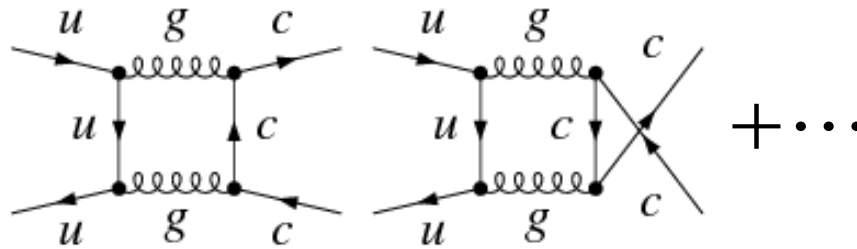


2) $gg \rightarrow c\bar{c}g$

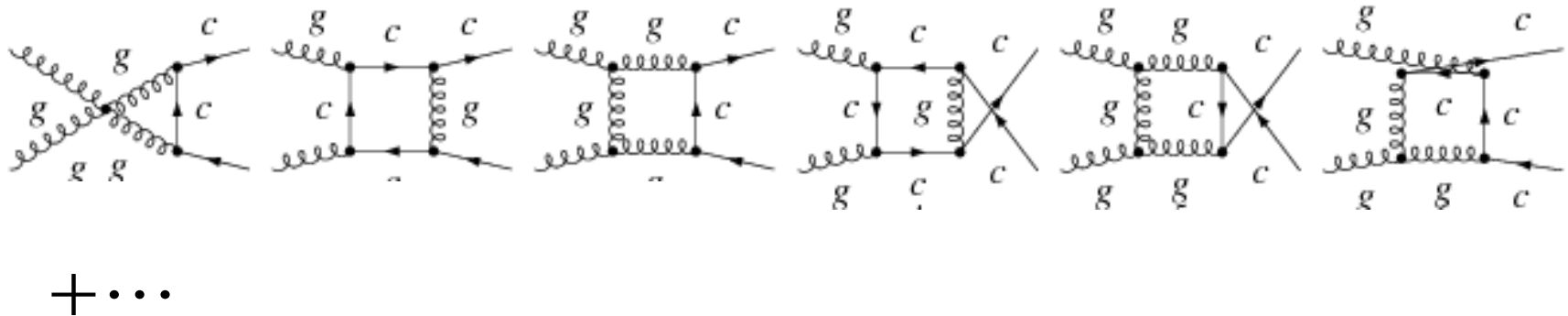


Virtual corrections to leading-order diagrams

1) $q\bar{q} \rightarrow c\bar{c}$

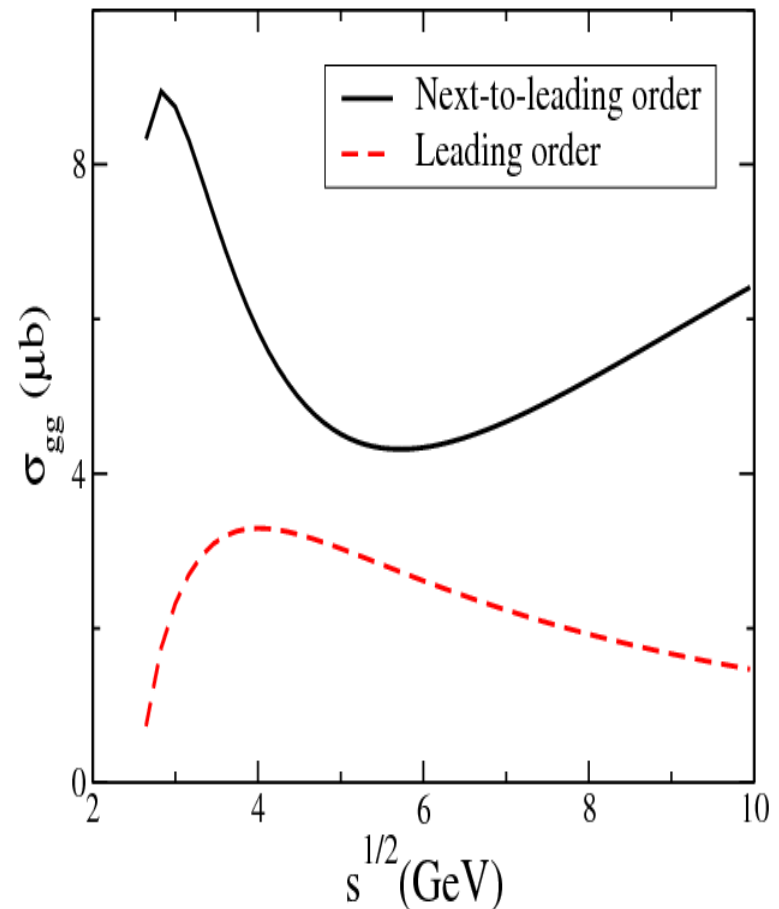
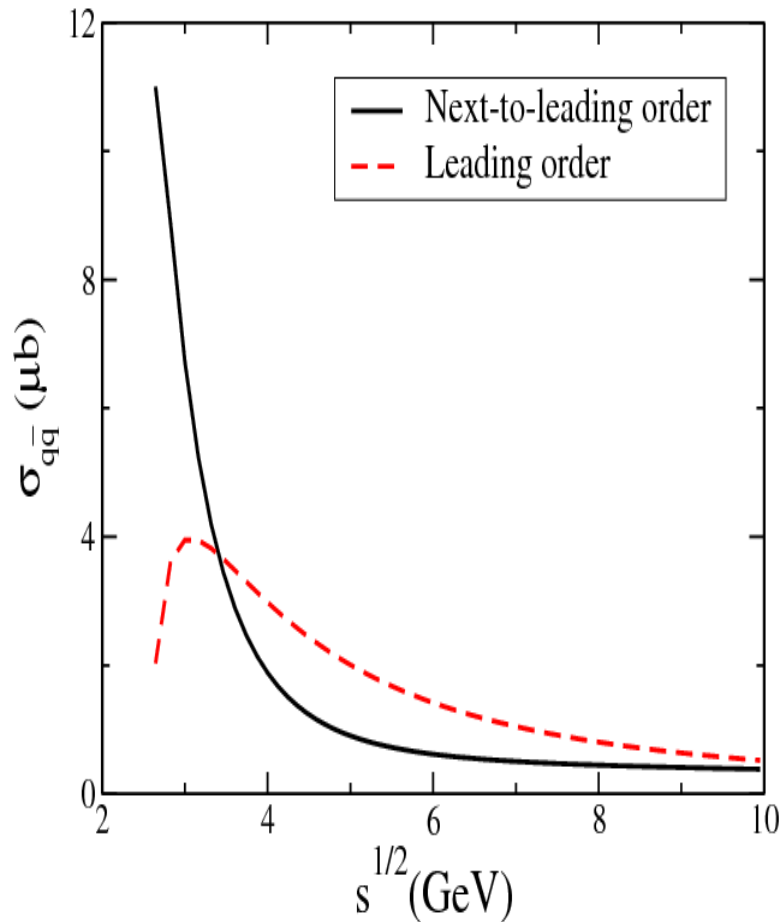


2) $gg \rightarrow c\bar{c}$



Charm quark production cross sections

P. Nason, S. Dawson & R.K. Ellis, NPB 303, 607 (1988)



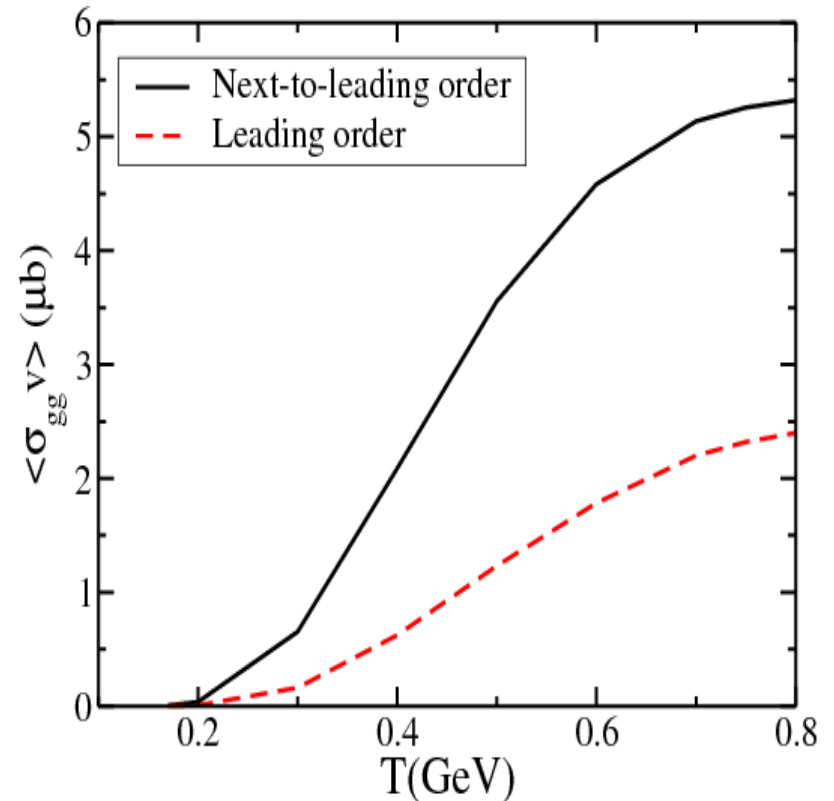
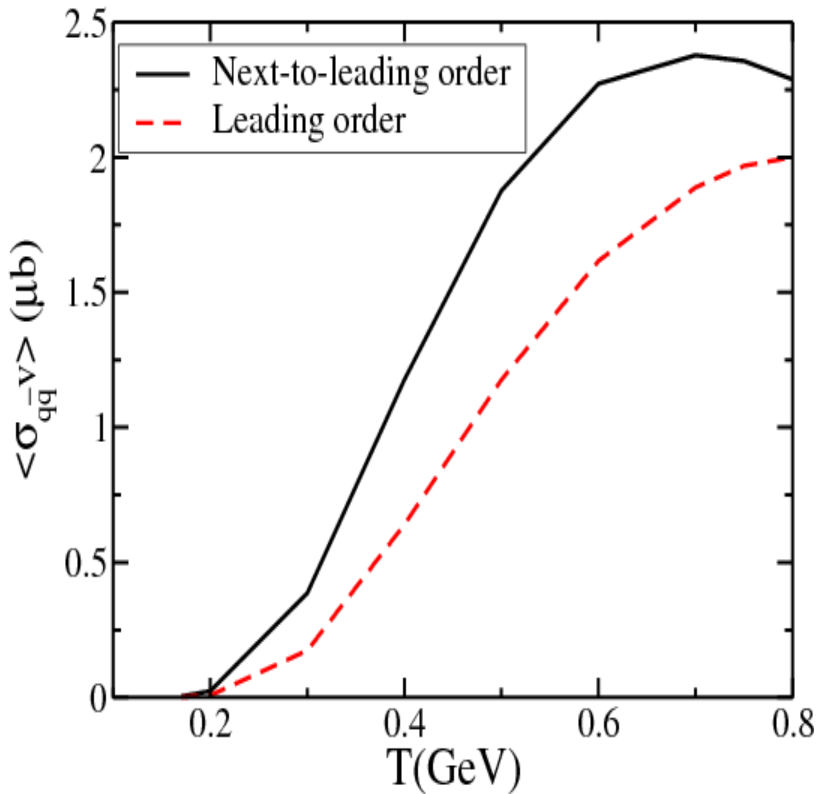
Next-to-leading order generally gives a larger cross section than the leading order except in $q\bar{q}$ annihilation at high energies.

Thermal averaged charm production cross sections

$$\langle \sigma_{ab \rightarrow cd} v \rangle = \frac{\int d^3 p_a d^3 p_b f_a(p_a) f_b(p_b) \sigma_{ab \rightarrow cd} v}{\int d^3 p_a d^3 p_b f_a(p_a) f_b(p_b)}$$

Thermal masses

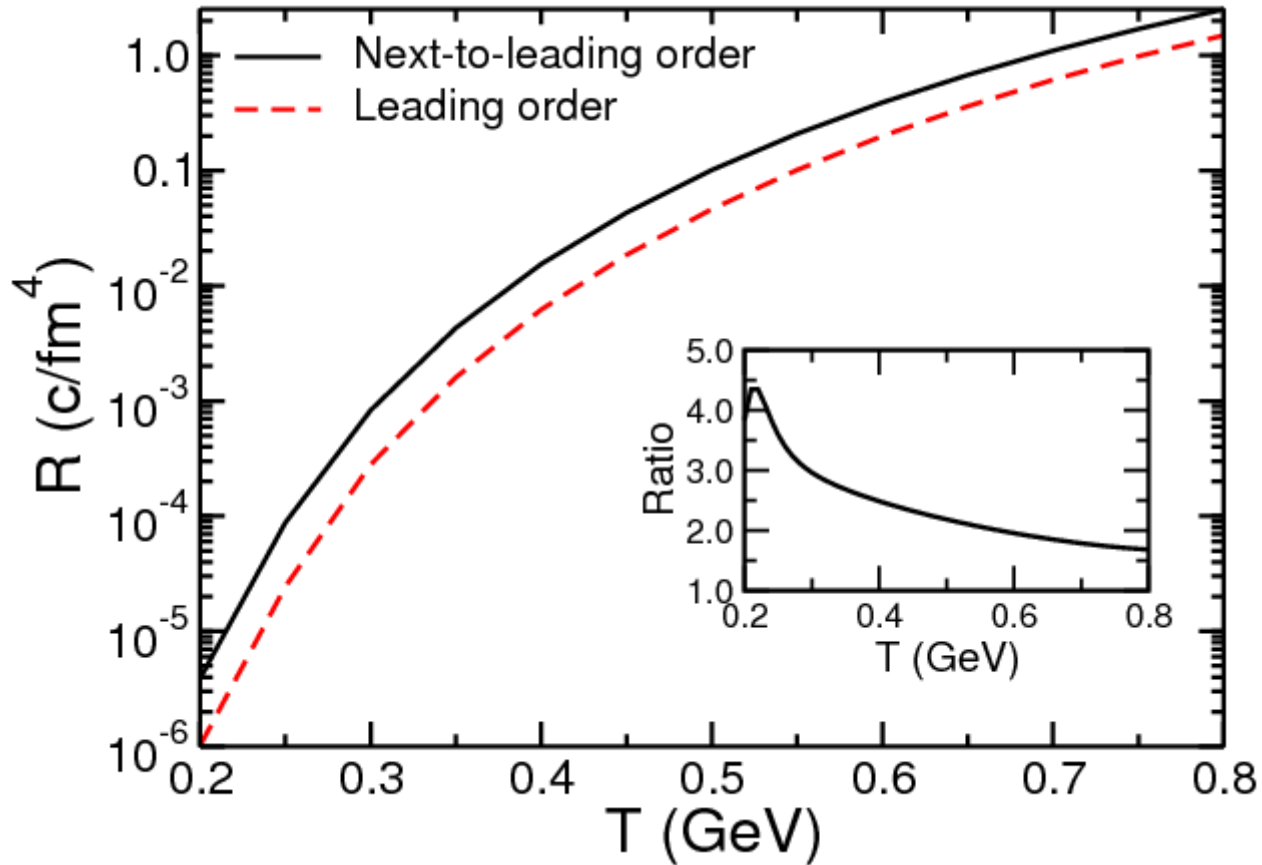
$$m_q = \frac{gT}{\sqrt{6}}, \quad m_g = \frac{gT}{\sqrt{2}}$$



Thermal averaged cross sections are larger in next-to-leading order, particularly in the gg channel. Slightly smaller if using massless partons.²⁶

Charm production rate

$$R = \left[\langle \sigma_{q\bar{q} \rightarrow c\bar{c}} \mathbf{v} \rangle + \langle \sigma_{q\bar{q} \rightarrow c\bar{c}g} \mathbf{v} \rangle \right] n_q^{\text{eq}} n_{\bar{q}}^{\text{eq}} + \frac{1}{2} \left[\langle \sigma_{gg \rightarrow c\bar{c}} \mathbf{v} \rangle + \langle \sigma_{gg \rightarrow c\bar{c}g} \mathbf{v} \rangle \right] (n_g^{\text{eq}})^2$$



Production rate increases exponentially with temperature

Rate equation for charm production from QGP

$$\frac{1}{V} \frac{dN_{c\bar{c}}}{d\tau} \approx \left[\left(\langle \sigma_{q\bar{q} \rightarrow c\bar{c}} \mathbf{v} \rangle + \langle \sigma_{q\bar{q} \rightarrow c\bar{c}g} \mathbf{v} \rangle \right) n_q^{\text{eq}} n_{\bar{q}}^{\text{eq}} + \frac{1}{2} \left(\langle \sigma_{gg \rightarrow c\bar{c}} \mathbf{v} \rangle + \langle \sigma_{gg \rightarrow c\bar{c}g} \mathbf{v} \rangle \right) (n_g^{\text{eq}})^2 \right] \left[1 - \left(\frac{n_{c\bar{c}}}{n_{c\bar{c}}^{\text{eq}}} \right)^2 \right]$$

QGP fire-cylinder dynamics at LHC

- Longitudinally boost invariant and transversely accelerated \rightarrow volume

$$V(\tau) = \pi \left[R_0 + \frac{a}{2} (\tau - \tau_0)^2 \right]^2 \tau$$

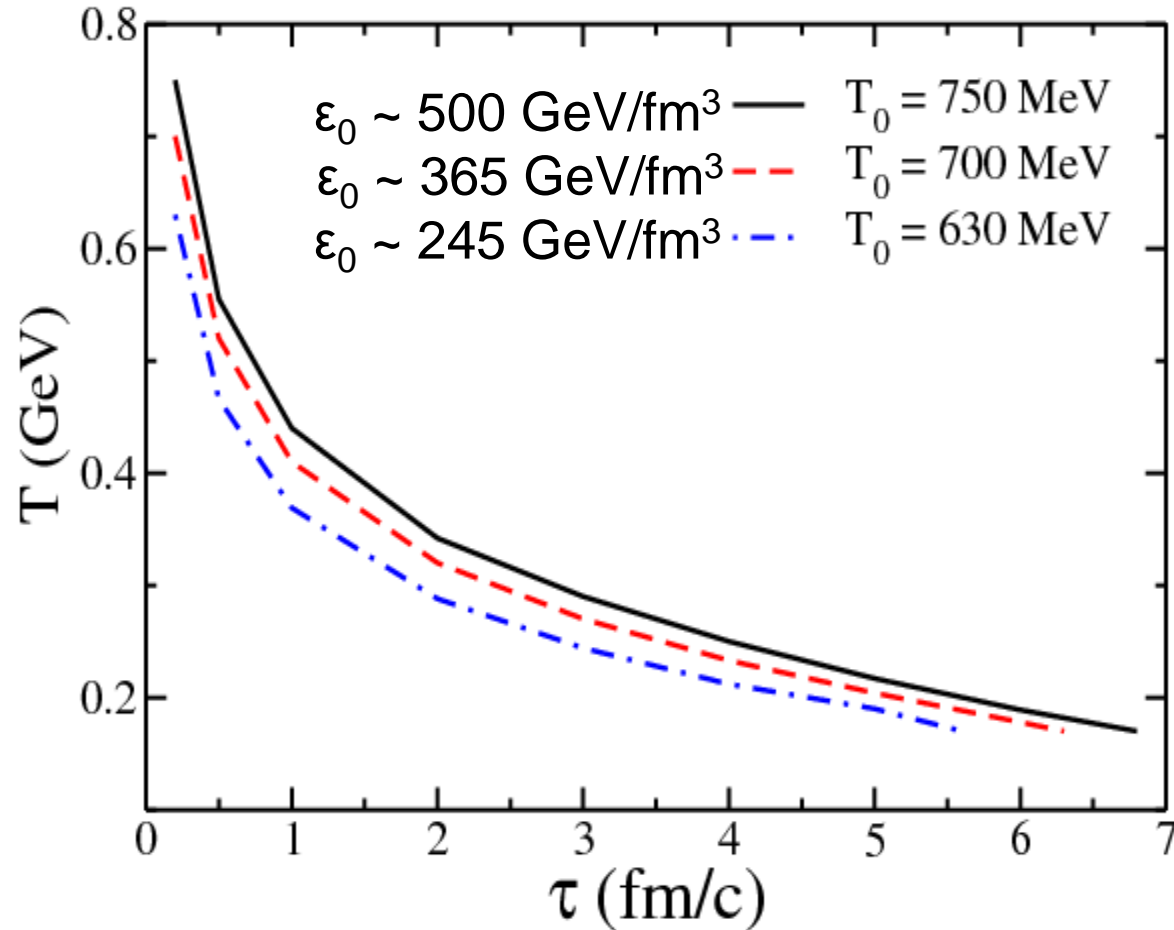
- For Pb+Pb @ 5.5 ATeV, $R_0 \sim 1.2 A^{1/3} \sim 7$ fm
- Expecting the QGP formation time τ_0 to be less than ~ 0.5 fm/c at RHIC, we take $\tau_0 = 0.2$ fm/c
- Taking transverse acceleration $a=0.1$ c²/fm, similar to that at RHIC

Initial temperature of QGP formed in HIC

- Color glass condensate: T. Lappi, PLB 643, 11 (2006)
 - At LHC, energy density at $\tau = 0.07 \text{ fm}/c$: $\varepsilon \sim 700 \text{ GeV}/\text{fm}^3$
 - Assuming ε decreases with time as $1/\tau \rightarrow \varepsilon_0 \sim 245 \text{ GeV}/\text{fm}^3$ at $\tau_0 = 0.2 \text{ fm}/c$
 - Using $\varepsilon \sim (T/160)^4 \text{ GeV}/\text{fm}^3 \rightarrow T_0 \sim 633 \text{ MeV}$ at LHC
 - At RHIC, $\varepsilon \sim 130 \text{ GeV}/\text{fm}^3$ at $\tau = 0.1 \text{ fm}/c \rightarrow T_0 \sim 361 \text{ MeV}$ at $\tau_0 = 0.5 \text{ fm}/c$
 - Uncertainty is , however, large due to Q_s^4 dependence
- HIJING (Gyulassy and Wang) or AMPT: Lin et al., PRC 72, 064901 (2005)
 - Initial transverse energy $dE_T/dy \sim 3000 \text{ GeV}$ at LHC
 - $$\varepsilon_0 \approx \frac{dE_T/dy}{\pi R_0^2 \tau_0} \approx \frac{3000}{3 \times 4.7^2 \times 0.2} \approx 226 \text{ GeV}/\text{fm}^3 \rightarrow T_0 \approx 620 \text{ MeV}$$
 - At RHIC, $dE_T/dy \sim 1000 \text{ GeV} \rightarrow \varepsilon_0 \sim 33 \text{ GeV}/\text{fm}^3 \rightarrow T_0 \sim 383 \text{ MeV}$ at $\tau_0 = 0.5 \text{ fm}/c$

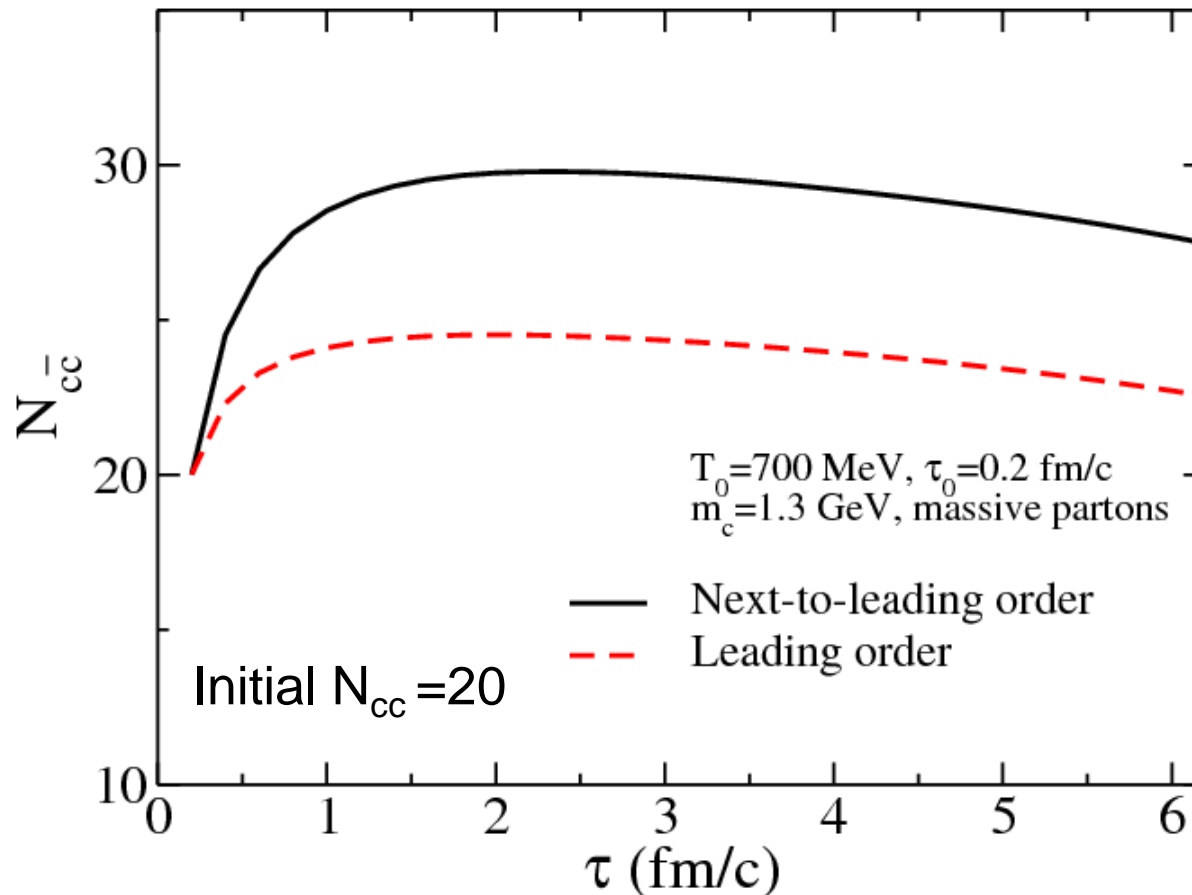
Temperature evolution at LHC

Entropy conservation \rightarrow



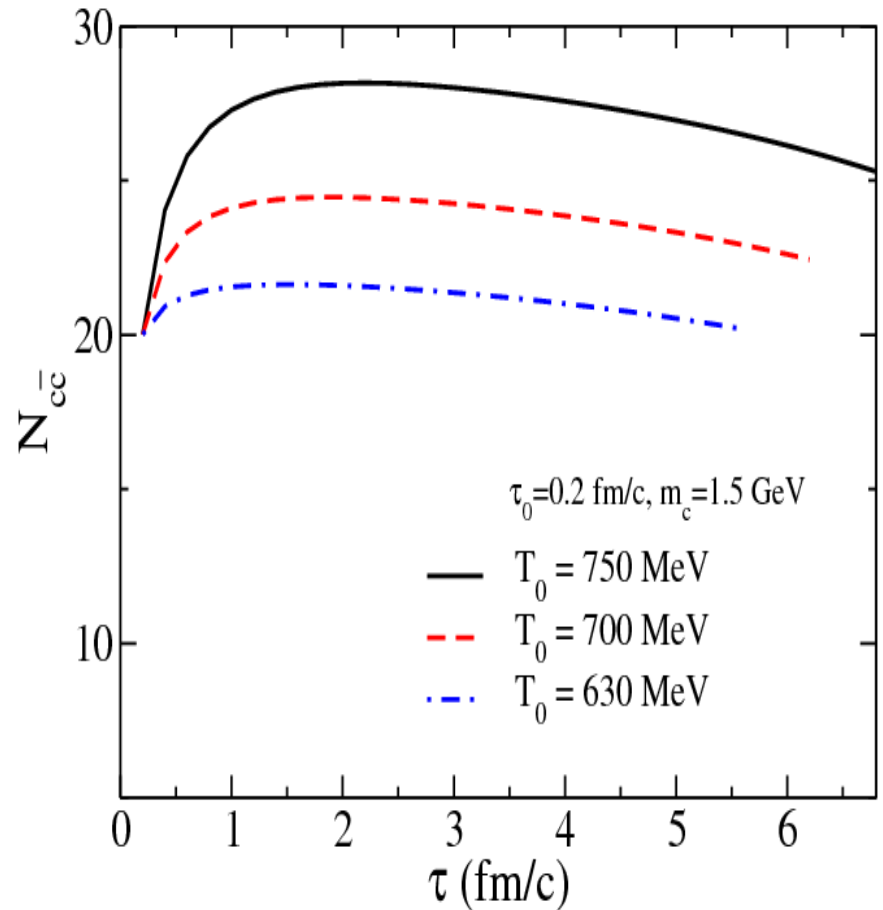
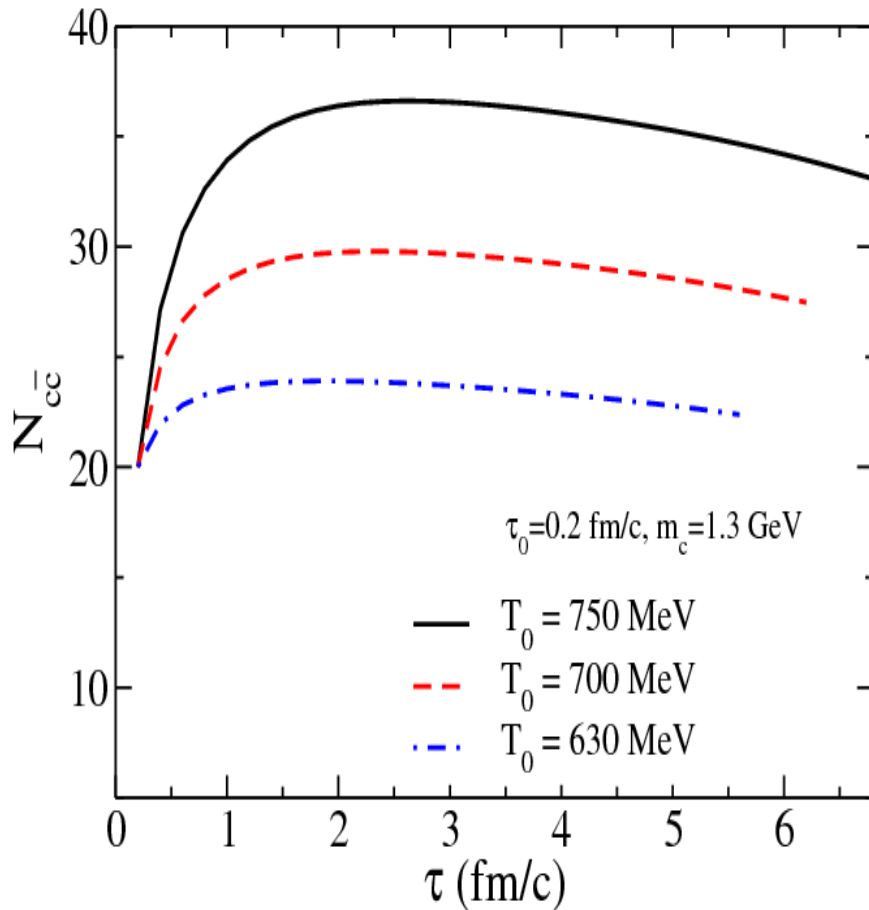
High temperature only exists briefly during early stage of QGP

Time evolution of charm quark pair at LHC



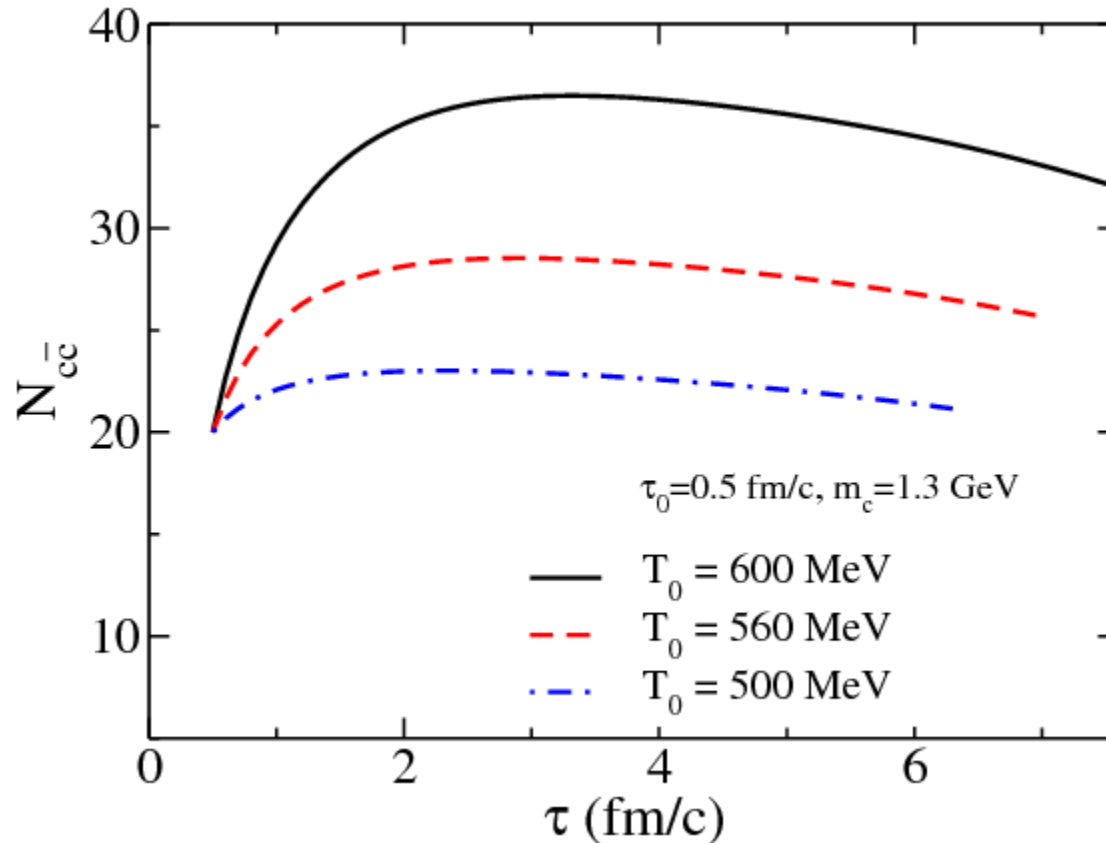
- Charm production in next-to-leading order is more than a factor of two larger than in the leading order
- Results using massless gluons are slightly larger

Initial temperature and charm quark mass dependence of thermal charm production



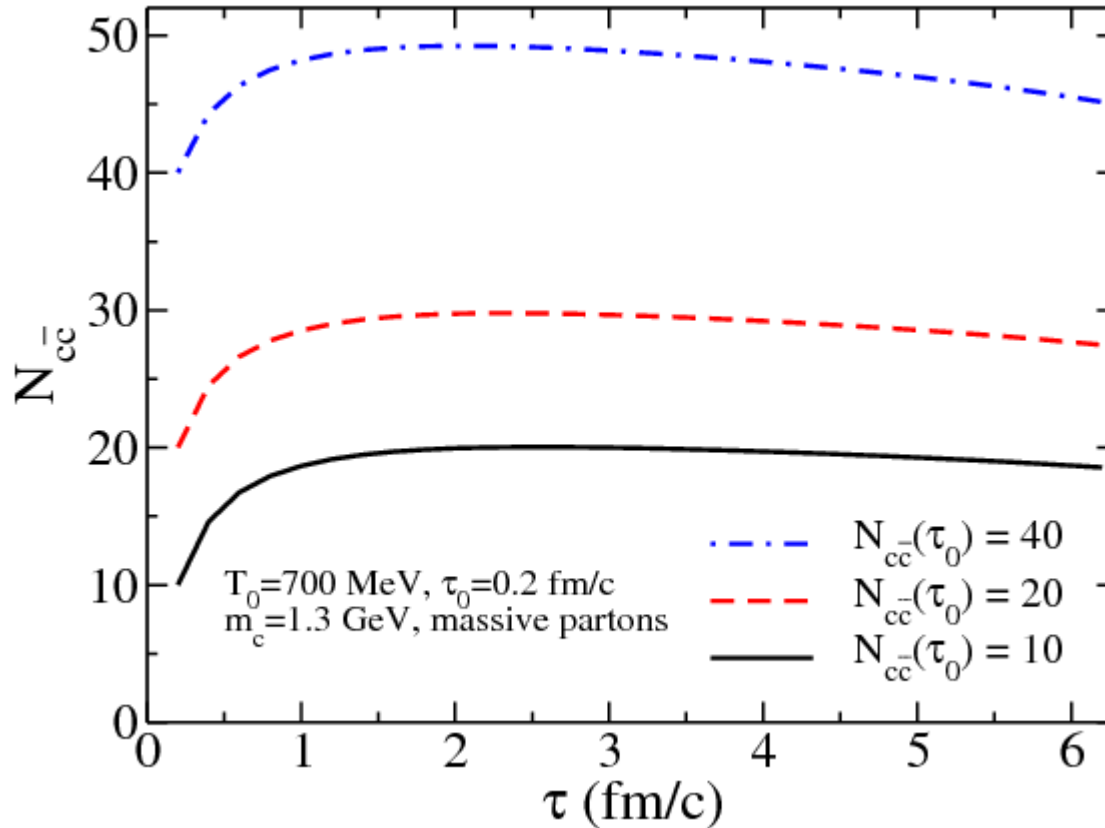
Increases with initial temperature but decreases with charm quark mass.

Charm production at LHC for $\tau_0=0.5$ fm/c



Similar results as $\tau_0 = 0.2$ fm/c , although initial temperature is lower

Dependence of charm production on initial charm abundance

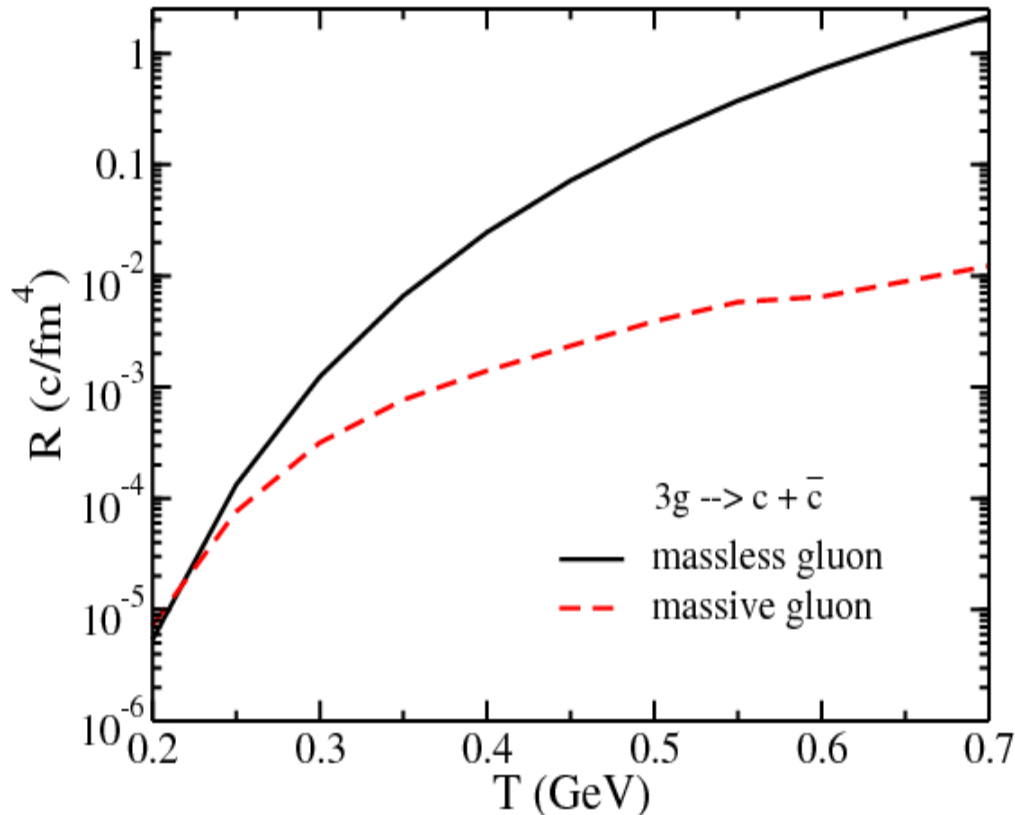


Thermal production becomes more important if initial charm abundance is small

Charm production from three-gluon interaction $ggg \rightarrow c\bar{c}$

Determine rate for $ggg \rightarrow c\bar{c}$ from $c\bar{c} \rightarrow ggg$ via detailed balance

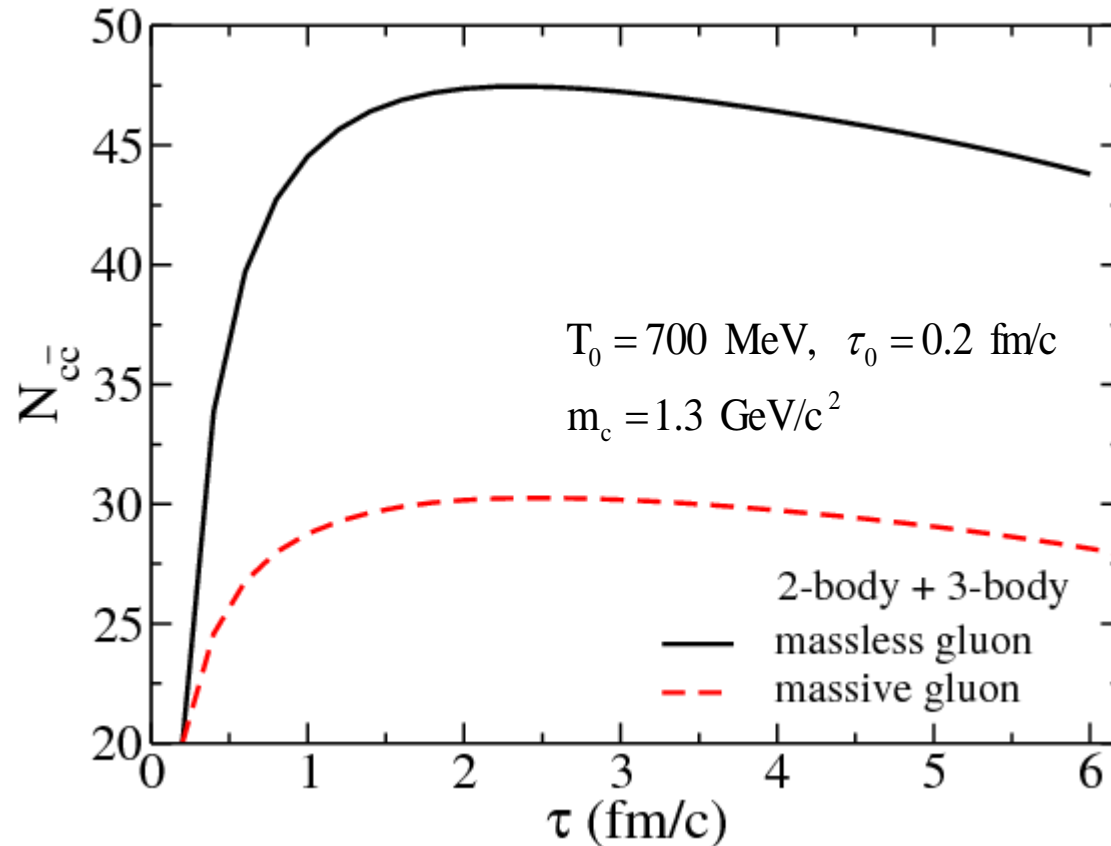
$$R \propto \frac{1}{3} \int \prod_{i=1}^5 d^3 p_i f_i(p_i) |M_{ggg \rightarrow c\bar{c}}|^2 \delta^{(4)}(p_1 + p_2 + p_3 - p_4 - p_5) \propto \langle \sigma_{c\bar{c} \rightarrow ggg} v \rangle n_c^{\text{eq}} n_{\bar{c}}^{\text{eq}}$$



Gluon density $\sim 0.5/\text{fm}^3$ at T_c
and much larger initially

- Negligible rate for massive gluons as the threshold becomes larger than the charm pair mass
- With massless gluons, the rate is comparable to that of two-body processes

Time evolution of charm quark pairs at LHC including both two- and three-body interactions



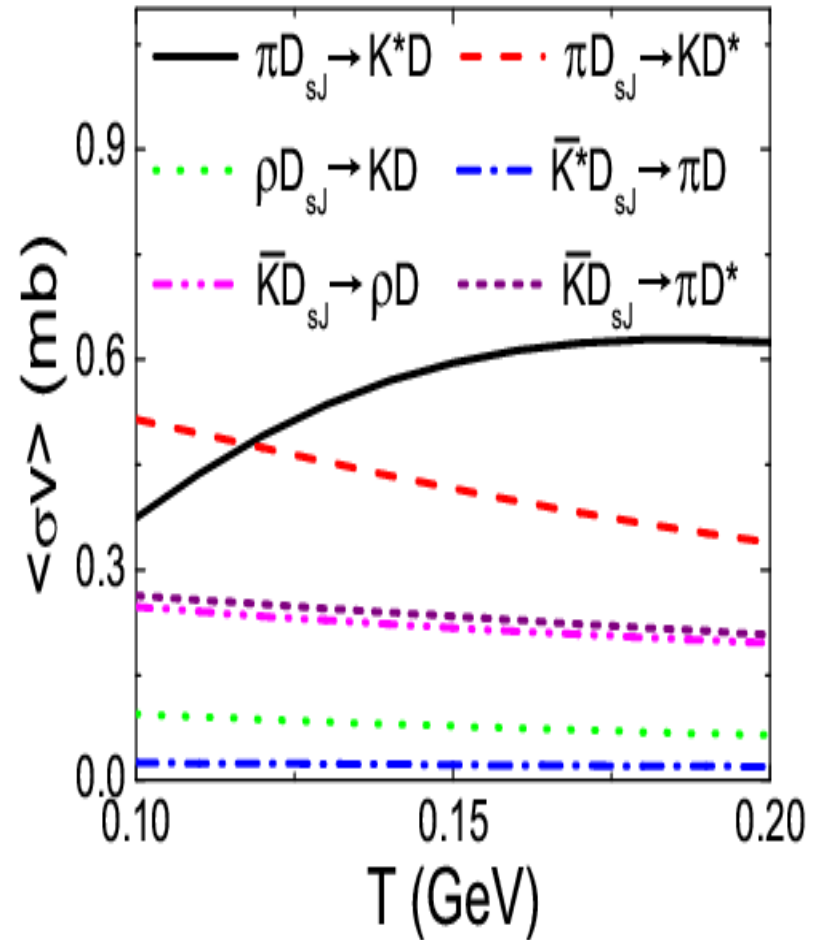
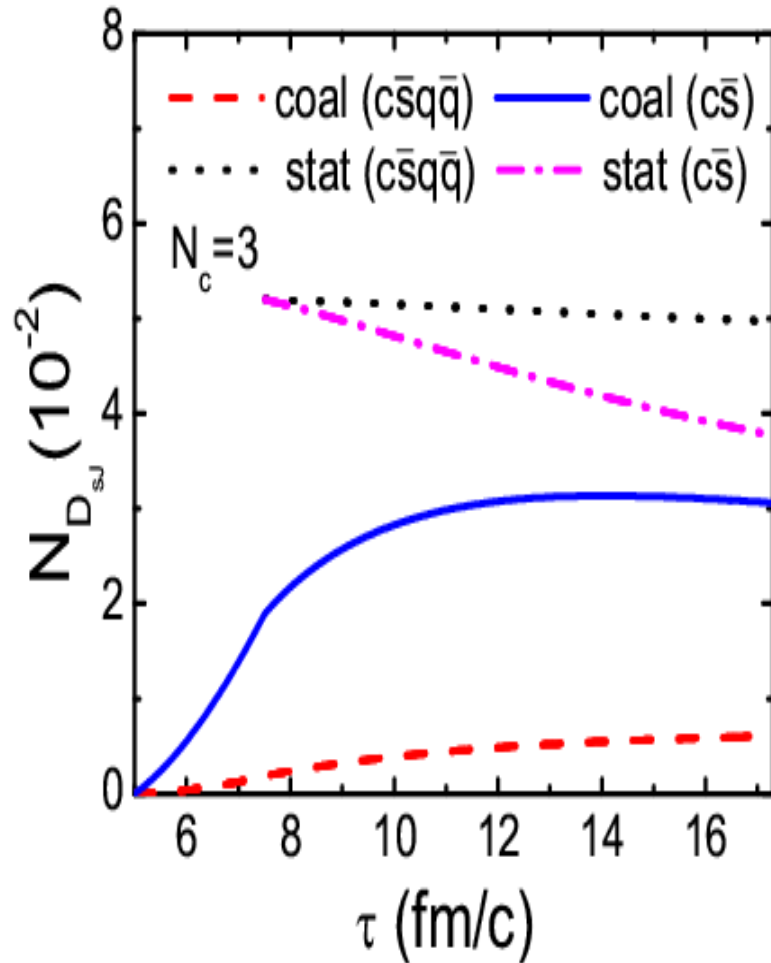
Significant thermal production of charms from QGP of massless gluons

Summary II

- Thermal charm production rate increases ~ exponentially with the temperature of QGP.
- Next-to-leading order enhances thermal production rate by more than a factor of 2.
- Charm production from three-gluon interactions is important if gluons are massless.
- Thermal charm production could be important at LHC.
- Understanding thermal charm quark production is important for understanding charmonium production in HIC.
- LHC provides the possibility to search for charmed exotics such as charmed tetraquark mesons and pentaquark baryons.

D_{sJ} production at RHIC

Chen, Liu, Nielsen, Ko, PRC 76, 064903 (2007))



Final yield is sensitive to the quark structure of D_{sJ}

- Charm tetraquark mesons
 - $T_{cc} (u\bar{d}\bar{c}\bar{c})$ is ~ 80 MeV below $D+D^*$ according to quark model
 - Coalescence model predicts a yield of $\sim 5.5 \times 10^{-6}$ in central Au+Au collisions at RHIC and $\sim 9 \times 10^{-5}$ in central Pb+Pb collisions at LHC if total charm quark numbers are 3 and 20, respectively
 - Yields increase to 7.5×10^{-4} and 8.6×10^{-3} , respectively, in the statistical model

- Charmed pentaquark baryons
 - $\Theta_{cs}(u\bar{d}us\bar{c})$ is ~ 70 MeV below $D+\Sigma$ in quark model
 - Yield is $\sim 1.2 \times 10^{-4}$ at RHIC and $\sim 7.9 \times 10^{-4}$ at LHC from the coalescence model for total charm quark numbers of 3 and 20, respectively
 - Statistical model predicts much larger yields of $\sim 4.5 \times 10^{-3}$ at RHIC and $\sim 2.7 \times 10^{-2}$ at LHC

Summary III

- Yield of D_{sJ} in HIC is sensitive to its quark structure
- Enhanced charm production at LHC makes the latter a possible factory for studying charmed exotics
- Because of quark number scaling of hadron elliptic flow (coalescence model), i.e., $v_2(p_T/n)/n$ is universal, study of the elliptic flows of charm exotics in HIC provides the possibility to verify their quark structure.